Title

Developing an in vitro thermal shift assay to assess target engagement of spliceosome inhibitors

Author

Amorello, Angela Nicole

Publication Date

2023

Peer reviewed|Thesis/dissertation

UNIVERSITY OF CALIFORNIA

SANTA CRUZ

Developing an *in vitro* thermal shift assay to assess target engagement of spliceosome inhibitors

A dissertation submitted in partial satisfaction

of the requirements for the degree of

DOCTOR OF PHILOSOPHY

in

CHEMISTRY

by

Angela N. Amorello

September 2023

The Dissertation of Angela N. Amorello is

approved:

Professor Melissa S. Jurica, Chair

Professor Manuel Ares, Jr.

Professor Michael Stone

Peter F. Biehl
Vice Provost and Dean of Graduate Studies

Table of contents

List of Figures

Chapter I: Introduction

Chapter II: Thermal shift assay to measure native SF3B inhibitor binding

Chapter III: U2 snRNP Interactions with an intron

Abstract

Angela Nicole Amorello

Developing an *in vitro* thermal shift assay to assess target engagement of spliceosome inhibitors

Successful human gene expression requires a balance of flexibility and accuracy. Human genes are transcribed as pre-mRNAs that contain coding exon sequences interspersed with non-coding intron sequences. Introns must be removed, and exons joined together to produce a functional mRNA by pre-mRNA splicing. Splicing is catalyzed by a ribonucleoprotein molecular machine called the spliceosome. The spliceosome is a complex enzyme with many key players and assembles piece-by-piece on each pre-mRNA. Accurate splicing requires identification of the intron/exon boundaries by the spliceosome. The spliceosome relies on identifying introns by unique sequence signatures. Poor conservation of these sequences in human introns affords the spliceosome flexibility for alternative splicing, but also necessitates tight regulation. My research focuses on U2 snRNP and its associated protein subcomplex SF3B, which are involved in branch point sequence recognition. I speculate that branch point sequence recognition by U2 snRNP in humans is reliant on SF3B-mediated interactions. I used two approaches to interrogate SF3B-mediated interactions, 1) assessing how drug binding impacts the thermal stability SF3B protein, SF3B1 and 2) determining whether SF3B1-interacting partner, U2AF is required for intron recognition.

Dedication

I dedicate this work to my mother and father. Without their love and support, this would not be possible. I love you both. Thank you! This work is also dedicated to Black scientists of the past, the present and the future. I also dedicate this to uncles Karl and Kenny Craig.

Acknowledgments

I am overwhelmingly grateful for my PI, Dr. Melissa Jurica, who believed in me, especially during times I did not believe in myself. I have this problem, where I'm afraid of everything. I still am, but no longer, when it comes to science. I attribute this newfound courage to Melissa. If I could do graduate school over again, I would choose her as my PI time and again. She sincerely cares about every student that she mentors, as much as she cares about science. I am fortunate to have had such a supportive mentor. Thank you for always being here for me and reminding me what I can be capable of.

To the Jurica lab, who supported me and helped me grow in ways I never knew were possible, thank you. I am especially grateful for Beth Prichard, Veronica Urabe, Hannah Maul-Newby, and Meredith Stevers. All the laughs, all of our West End Tap happy hours, and all of the love will forever be invaluable to me. Thank you.

My committee members, Dr. Manuel Ares and Dr. Michael Stone, have been very supportive and have provided insightful feedback throughout the years, which I am immensely grateful for.

Lastly, I am beyond grateful for my close friends and family, for being my lifeline during this journey. Shout out to Jess, Murs, Messina, Piits, Justyn, and Cassandra. Y'all are everything to me. To all of the great friends that I made here in Santa Cruz, who let me be me, thank you! I am also extremely grateful to Jake, who supported me during the most stressful year of grad school. I love you.

Chapter I: Introduction

Central Dogma

The central dogma offers a simplified view of the genetic flow of information, stating that DNA is transcribed into mRNA, which can be translated into proteins. However, eukaryotic gene expression requires additional RNA processing steps (Fig. 1.1). In the nucleus, nascent RNAs are modified co-transcriptionally at their 5′ end via a 5′ -5′ reverse triphosphate linkage with the N7-methylated guanosine cap structure (Shatkin et al. 1976, Moteki et al. 2002). Capping of mRNA is required for initiating protein synthesis, offers protection from 5′ to 3′ exonuclease cleavage, and helps recruit protein factors for other RNA processing steps (Topisirovic et al. 2010). Eukaryotic transcripts contain coding sequences called exons interrupted by non-coding sequences, termed introns that require removal to produce a mature mRNA. Intron sequences are excised, and exon sequences subsequently joined together in an essential RNA process called pre-mRNA splicing (Berget et al. 1977; Chow et al. 1977). Splicing will be discussed in more detail throughout this dissertation. After successful 5′ end capping and pre-mRNA splicing, nearly all protein coding mRNAs are polyadenylated with about 200 adenosines (Coolgan and Manley et al. 1997). Finally, when key RNA-binding proteins declare that an mRNA is fully processed, it will be exported from the nucleus into the cytoplasm.

Pre-mRNA Splicing

Pre-mRNA splicing relies on signatures within the intron (Fig 1.2) to accurately differentiate between intron and exon sequences. These signatures, which are highly conserved in yeast, include the 5′ and 3′ splice site and the branch

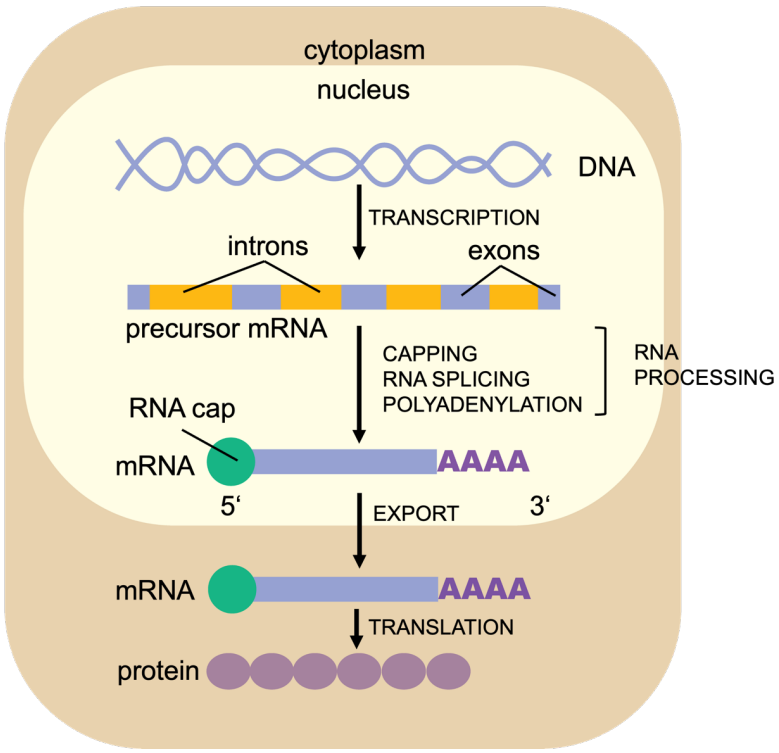

Figure 1.1. Central Dogma and RNA processing.
Diagram of the central dogma expanded to reflect RNA processing steps required for eukaryotic gene expression (Adapted from Alberts et al., Molecular Biology of the Cell 6th Edition. 2015)

point sequences. The consensus 5′ splice site and 3′ splice site and branch point sequences are **GU**AUGU (Burge et al. 1999), **AG** (Mount et al. 1982), and UACUA**A**C (Langford and Gallwitz, 1983, Zhuag et al.,1989) respectively. In humans, the 3′ splice site is preceded by a stretch of pyrimidines called the polypyrimidine tract immediately downstream of the branch point sequence. Distance between the branch point sequence and the 3′ splice site is typically 18-40 nucleotides. Conservation of these sequences, including the branch point sequence, is greatly reduced in human introns. Human branch point sequences generally have a yUn**A**y motif (Gao et al. 2008) but vary considerably. In addition to divergent branch point sequences, human genes have long introns, which together creates equivalency among branch point sequence

candidates. Weaker splicing signals likely afford human genes the flexibility to be alternatively spliced. The majority of human genes are alternatively spliced to produce multiple mRNA isoforms from the same transcript, greatly increasing proteome diversity (Lee and Rio 2015).

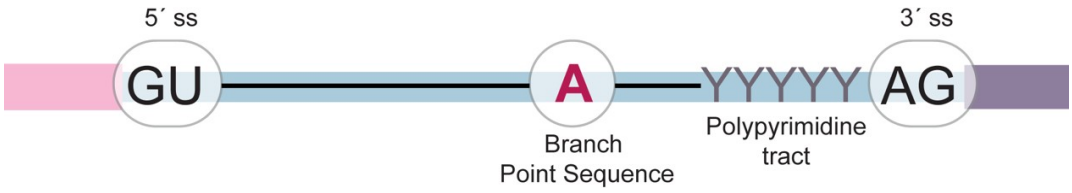

Figure 1.2 Intron Landmarks
Schematic of a pre-mRNA highlighting intronic splicing signals, including the 5′ and 3′ splice sites, branch point sequence, and polypyrimidine tract. 5′ and 3′ exons are represented by pink and mauve boxes respectively.

The Spliceosome

Splicing is catalyzed by a multi-megadalton molecular machine called the spliceosome comprised of five Uridine-rich small nuclear RNAs that with their core proteins form ribonucleoproteins (snRNPs). In addition to snRNPs, hundreds of proteins join and leave the spliceosome, as the result of many dynamic structural rearrangements (Fig. 1.3) occurring throughout splicing (Will and Lürhmann, 2011). The spliceosome assembles piece-by-piece on each pre-mRNA destined for splicing. U1 snRNP base-pairs with the 5′ splice site (Lerner et al., 1980), while SF1 and the U2AF heterodimer bind the branch point sequence, polypyrimidine tract and 3′ splice site respectively forming E complex (Selenko et al., 2011). During the transition from E-to-A complex, U2 snRNP defines the intron/exon boundary through recognition of the branch point sequence in incompletely understood, ATP-dependent process. After intron boundaries are delineated, the U4/U6.U5 tri-snRNP joins forming B complex,

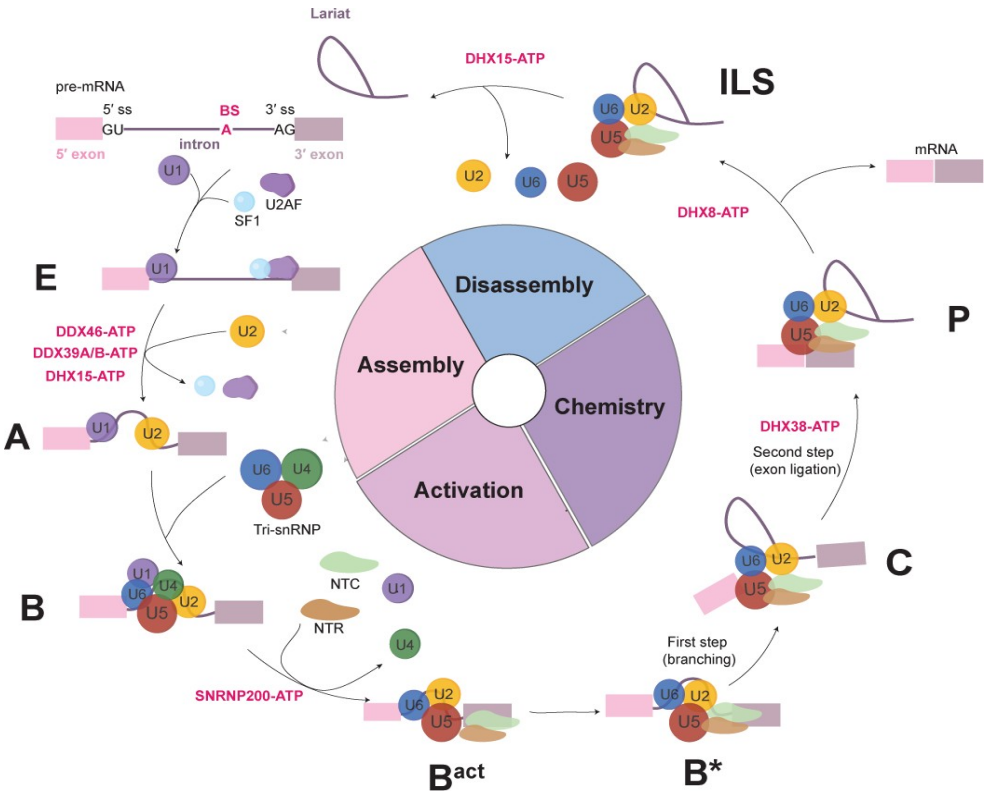

Figure 1.3 Splicing Cycle
Splicing cycle depicting the different stages of the splicing reactions, spliceosome components, and the complexes that result from dynamic structural rearrangements (Adapted from Shi et al., 2017)

which becomes activated for first-step chemistry following many structural rearrangements including the unwinding of U4/U6 snRNP and the departure of U1 and U4 snRNP (B^{act}) (Will and Lürhmann, 2011). Following first step chemistry, further rearrangements yield C complex, which will catalyze exon ligation. Generally, these structural rearrangements are orchestrated by RNA-dependent helicases and are dependent on NTP hydrolysis or binding.

Splicing Chemistry

Pre-mRNA splicing consists of two transesterification reactions called branching and exon ligation (Fig. 1.4). During the branching reaction the 2′-hydroxyl of the invariant

branch point adenosine launches a nucleophilic attack on the 5′ splice site producing the 5′ exon and 3′ exon-intron lariat intermediate. Next exon ligation is achieved by nucleophilic attack of the 3′ splice site phosphate by the 3′-hydroxyl group of the 5′ exon ligating the exons and releasing the intron. Although the spliceosome has 100s of proteins, it is a ribozyme. Splicing chemistry is catalyzed by U2 and U6 small nuclear RNAs (Fica et al. 2013).

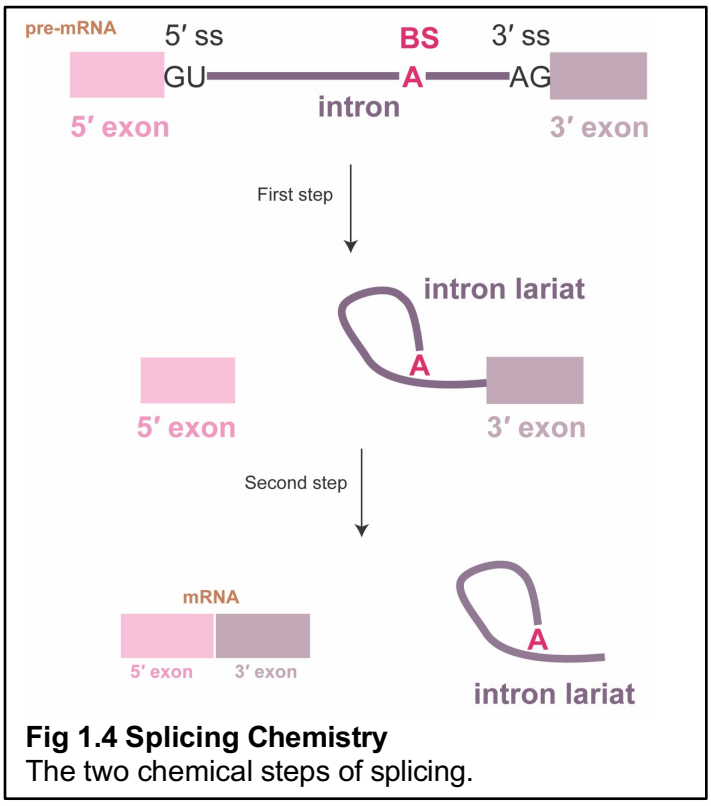

Fig 1.4 Splicing Chemistry
The two chemical steps of splicing.

U2 snRNP

Spliceosome component, U2 snRNP, defines the intron boundaries through ATP-dependent recognition of the branch point sequence (Matera and Wang, 2014). U2 snRNP exists in two forms, 12S and 17S, the latter being the functional snRNP (Fig. 1.5). 12S U2 snRNP comprises the U2 snRNA and core proteins A′ and B″, while 17S U2 snRNP additionally contains SF3A and SF3B protein subcomplexes (Behrens

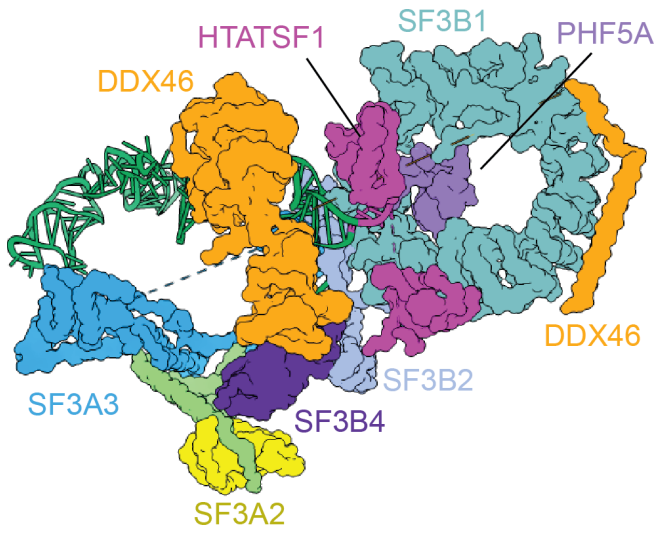

PDB: 6Y5Q

Figure 1.5. U2 snRNP
Structural model of 17S U2 snRNP adapted from Zhang et al., 2020.

et al., 1993, Behzadnia et al., 2006). U2 snRNP identifies the branch point sequence by a not fully resolved mechanism. Branch point sequence choice can determine which 3′ splice site is used, and thus the mRNA produced (Luukonen et al., 1997), which has biological consequences, and must be tightly regulated. Recognition of the branch point sequence by U2 snRNP involves base-pairing between the branch point interacting step loop (BSL) and branch point sequence. Given the variance of branch point sequence contenders in human genomes, base-pairing is likely insufficient to ensure splicing fidelity. U2 snRNA/pre-mRNA base-pairing is likely supplemented with protein-RNA and protein-protein interactions (Gozani et al., 1998). Cancer cells reduce splicing fidelity by mutating splicing factors that recognize the branch point sequence. SF3B sub-complex component (Lee and Abdel-Wahab, 2016), SF3B1 helps recruit U2 snRNP to a branch point sequence seemingly via U2AF2/SF3B1 interactions (Gozani et al., 1998, Cretu et al., 2016). SF3B1 mutations are frequently detected

hematological malignancies, including chronic lymphocytic leukemia and myelodysplastic syndrome (De Kesel et al., 2022). Cancer-associated SF3B1 mutations result in alternative branch point sequence and 3′ splice site usage producing aberrant transcripts (Darman et al., 2015, Alsafadi et al., 2016).

SF3B Inhibitors

Natural products that display potent cytotoxicity towards tumor cells and mouse xenografts were identified in screens for anti-tumor compounds (Mizui et al., 2004, Sakai et al., 2002, Nakajima et al., 1996). Later, it was discovered that these compounds inhibit splicing through targeting SF3B activity (Kaida et al., 2007, Kotake et al., 2007, Hasegawa et al., 2011). These compounds stall spliceosome assembly prior to the ATP-dependent step of A complex assembly resulting in labile A-like complexes prone to disassembly (Corrionero et al. 2011, Roybal and Jurica et al. 2010). Although, structurally distinct, binding assays (Kotake et al. 2007, Kaida et al., 2007), competition assays (Effenberger et al. 2016, Lopez et al., 2021) and structural models (Cretu et al., 2018, Cretu et al., 2021) reveal that these compounds all bind SF3B1.

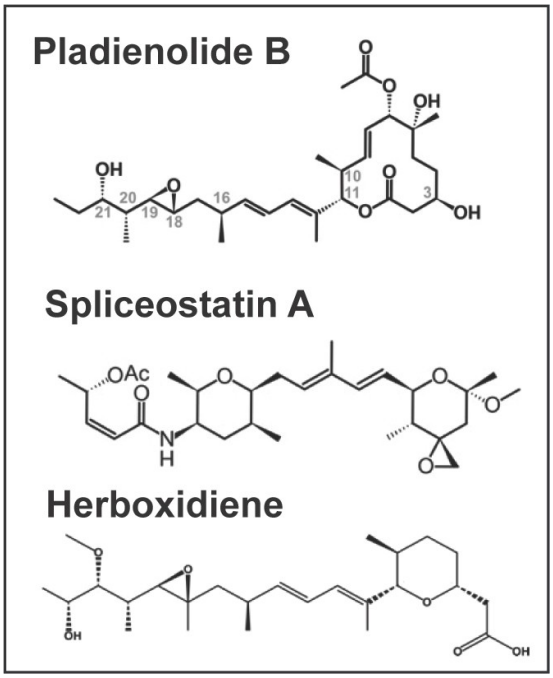

Figure 1.6 Spliceosome inhibitor structures.
Chemical structures of pladienolide B, spliceostatin A, and herboxidiene

Chapter II: Thermal shift assay to measure native SF3B inhibitor binding

Abstract

SF3B1, a core spliceosome component, is often mutated in cancer. The role of SF3B1 in pre-mRNA splicing is to accurately identify a branch point sequence in an intron to be excised, deciding the fate of the mRNA product. Three compounds that inhibit tumor cell growth were shown to inhibit splicing by targeting SF3B1 activity. Structure activity relationships identified analogs that do not inhibit splicing. However, some inactive analogs can compete with active inhibitors suggesting binding is not sufficient for activity. To better understand the mechanism of splicing inhibition by SF3B1-targetting inhibitors, we used an *in vitro* thermal shift assay with HeLa nuclear extract, to test the thermostability of SF3B1 in the presence of spliceosome inhibitors, herboxidiene, pladienolide B, and spliceostatin A or their inactive analogs. This assay exploits the principle that ligand binding increases the thermostability of their target proteins by inducing conformational changes. We observed that binding of spliceostatin A increases SF3B1 thermostability, suggesting that binding induces a stabilizing conformational change. Monitoring SF3B1-inhibitor engagement in this system allows to observe the interplay between SF3B1, its natural ligands, and spliceosome inhibitors.

Introduction

Eukaryotic genes are transcribed as precursor messenger RNAs (pre-mRNAs) with discontinuous sequences that encode genetic information, called exons, interrupted by non-coding sequences, called introns, that are removed by the process of pre-mRNA splicing. Splicing is catalyzed by a complicated and dynamic ribonucleoprotein (RNP) called the spliceosome. The spliceosome is composed five U-rich small nuclear RNAs (U1, U2, U4, U5 and U6 snRNAs) that with their associated proteins form RNPs called snRNPs (Wilkinson et al., 2019). Apart from snRNPs, the spliceosome has hundreds of proteins that join and leave in a series of structural rearrangements that occur throughout the splicing process. Spliceosomes assemble and function through a series of transient complexes. To initiate spliceosome assembly, intronic features, such as the 5′ and 3′ splice sites are identified by U1 snRNP and U2AF forming E complex (Figure 3.1 A). The spliceosome A complex forms with ATP-dependent recognition of the branch point sequence (BPS) by U2 snRNP (Kramer 1996, Staley and Guthrie, 1998). This step is crucial because, the branch point adenosine will initiate the first of two chemical steps of splicing through nucleophilic attack the 5′ splice site, which produces a free 5′ exon and 3′ exon-intron lariat intermediate (Will and Lürhmann et al., 2011). BPS recognition also influences the 3′ splice site choice that determines the exon-intron boundary.

U2 snRNP is composed of U2 snRNA and its core proteins (12S U2 snRNP), as well as SF3A and SF3B components and transient proteins like TatSF1(17S U2 snRNP) (Will et al. 2002). U2 snRNA base pairing with the BPS is considered the most important factor in branchpoint selection (Wu and Manley, 1989), but U2 snRNP proteins are also likely involved- particularly, SF3B1. SF3B1 is part of the SF3B

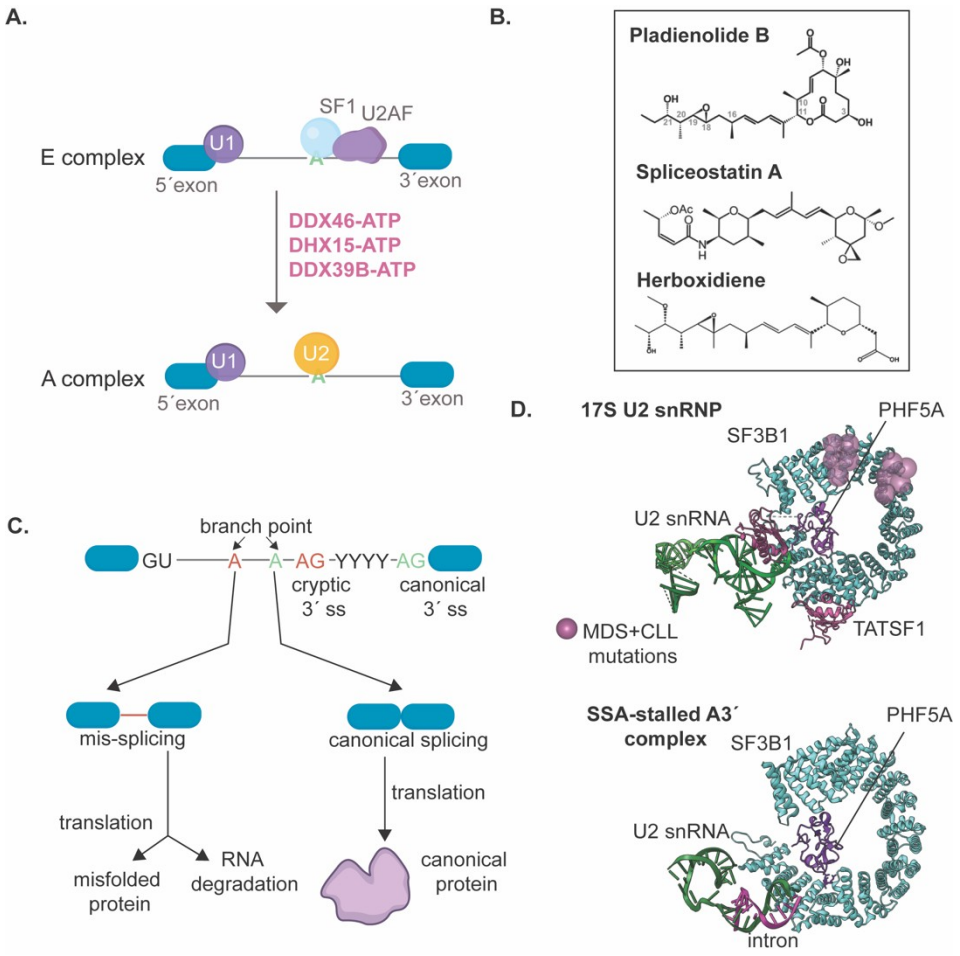

Figure 2.1. SF3B1 cancer mutations complicate branch point sequence selection
A) Schematic showing transition from E to A complex when U2 snRNP joins the intron. B) Cartoon representation of SF3B1 (Zhang et al. 2020) with locus of common MDS and CLL mutations indicated by magenta spheres (Cretu et al. 2016). C) Schematic depicting potential consequences of alternative branch point sequence and 3′ splice site use. D) Comparison of SF3B1 conformation in 17S U2 snRNP (PDB: 65YQ) and Spliceostatin A-Stalled A3′ complex (PDB: 7ONB)

complex that contacts sequences flanking the BPS in an ATP-dependent manner (Gozani et al. 1998). Whole exome sequencing of individuals with chronic lymphocytic leukemia (CLL) identified somatic mutations in SF3B1 (Quesada et al. 2011). Patients with SF3B1 mutations were more likely to have faster disease progression and a poorer prognosis (Quesada et al. 2011). SF3B1 mutations have also been identified

in myelodysplastic syndrome, as well as in breast and pancreatic cancers (Wan et al. 2013, Yoshida and Ogawa 2014). Analysis of transcriptome data from CCL, breast cancer, and uveal melanoma tumor samples reveal that their associated SF3B1 mutations result in usage of a non-canonical BPS and 3′ splice site pair producing aberrantly spliced transcripts (Darman et al. 2015, DeBoever et al. 2015) (Fig. 2.1C). Interestingly, the most frequently occurring SF3B1 mutation, SF3B1^{K700E} drives Myc hyperactivation via aberrant splicing (Liu et al. 2020). Further, interfering with splicing genetically or pharmacologically *in vivo* reduces viability and tumorigenicity in MYC-dependent breast cancers (Hsu et al., 2015). The crucial role of SF3B1 in splicing fidelity represents a vulnerability for anti-cancer therapeutics.

The SF3B complex was identified as a target for natural products pladienolide B (PB), herboxidiene (HB), and spliceostatin A (SSA) (Yokoi et al., 2011, Kaida et al., 2007), which display cytotoxicity and anti-tumor activity (Mizui et al., 2004, Sakai et al., 2002, Nakajima et al., 1996) (Figure 2.1B). Consistent with SF3B's role in BPS recognition, they impede spliceosome assembly during A complex formation. Although these compounds, collectively known as SF3B1 inhibitors, share a common target, many of their chemical features differ, raising the question of whether they have a conserved mechanism of action. Recent structural studies reveal that a common diene functionality that fits in a tunnel-like cavity between SF3B1 and the SF3B PHF5A protein. Comparison of recent structural models of the 17S U2 snRNP (Zhang et al. 2020) and drug-stalled splicing complexes (Cretu et al. 2018, Cretu et al. 2021) both display SF3B1 in an open conformation that appears to be stabilized by Tat-SF1 and spliceostatin A or Pladienolide B respectively (Fig. 2.1D). Drug-bound SF3B1 appears to be propped open with the branch point adenosine binding site occluded and unable

to associate with intron (Cretu et al. 2021). In contrast, a *Saccharomyces cerevisiae* A complex (aka prespliceosome) cryo-EM structure shows the N- and C- termini of SF3B1 coming together to stabilize the U2-BPS branch helix (Plaschka et al. 2018). These observations support a model where inhibitor and pre-mRNA binding are mutually exclusive and compete for an SF3B1 population that is in the open conformation.

Our group has carried out extensive structure activity relationship studies of SF3B1 inhibitors and identified chemical features required for splicing inhibition (Effenberger et al., 2014; Effenberger et al., 2016). Competition assays provide evidence that a herboxidiene analog that binds but does not inhibit splicing (iHB) competes with its active analog as well as with pladienolide B and spliceostatin A to rescue splicing inhibition, suggesting that 1) all compounds have a common pharmacophore and 2) that binding is not sufficient to interfere with SF3B1 function (Effenberger et al. 2014). The second result is surprising given the current model of SF3B1 inhibition. However, the assay used for these experiments did not directly assess binding.

In principle, the efficacy of any drug is contingent upon its ability to bind its target. Evidence from binding assays and structural models show that spliceosome inhibitors bind to purified SF3B complex and in U2 snRNP assembled into an A-like complex (Cretu et al. 2018, Cretu et al. 2021). Further, a streptavidin pull-down assay using biotinylated spliceostatin A confirmed that SF3B is a target for the compound (Kaida et al. 2007). However, this may not capture how these compounds interact with SF3B in its native environment. Unfortunately, monitoring SF3B1 inhibitor binding in cells or nuclear extract directly is not yet possible. However, it is possible to assess

whether a drug binds its target by treating cells or cell lysates with a compound and measuring its thermal stability (Molina et al., 2013). This biophysical method exploits the principle of ligand-induced stabilization of proteins. Thermal denaturation curves can be generated for purified proteins with measured thermal shifts at saturating ligand concentration and correlate with binding affinities determined by other methods. Molina and co-workers developed a thermal shift assay to measure drug interactions in a cells and cell lysates context (CETSA) wherein, aliquots of cell lysates are treated with drug and heated to a range of temperatures, followed by isolation of soluble protein by centrifugation (Jafari et al., 2014). For a protein to be well-suited to this assay, highly sensitive detection by its associated antibody is needed to measure subtle changes in the amount of protein in a sample. Further the protein must unfold cooperatively, being stable for some lower temperatures with a sharp decrease at an intermediate temperature.

In this study, I employ an *in vitro* thermal shift assay with HeLa nuclear extract to better understand how well splicing inhibitors engage with SF3B in its native environment. My findings indicate that SF3B1 exhibits a sigmoidal thermal denaturation profile following exposure to a range of increasing temperature. SF3B1 thermal stability is moderately impacted by binding of some spliceosome inhibitors. We also find that ATP-dependent conformational changes in SF3B have no detectable impact on SF3B thermal stability. By determining which splicing inhibitors productively engage with SF3B1 in nuclear extract, we can better understand which chemical features favor target engagement its natural environment, thus improving their clinical success.

Methods

HeLa Nuclear Extract Preparation

HeLa nuclear extract was prepared as previously detailed (Dignam et al. 1983) with HeLa S3 cells cultivated in DMEM/F-12 at a 1:1 ratio and 5% (v/v) newborn calf serum.

SF3B1 Thermal Shift Assay

HeLa nuclear extracts diluted to 50% (v/v) in Buffer E (20 mM Tris pH 7.9, 0.1 M KCl, 0.2 mM EDTA, 20% glycerol) were incubated with drug or vehicle for 10 minutes at 30 ºC. Following incubation, the nuclear extract was transferred into PCR tubes or a PCR plate in 10 µL aliquots. The PCR tubes or plate were heated temperatures ranging from 40-65 ºC for 3 minutes by thermal cycler. Heated samples were diluted to a final volume of 50 µL with cold Buffer E then transferred to 1.7 mL microfuge tubes. Insoluble protein was separated by centrifugation at 17,000 g for 30 minutes at 4 ºC. Supernatant containing soluble protein was transferred to new tubes and stored at -20 ºC for future analysis.

Quantitative Dot Blot

Milipore Immobilon® PVDF membrane (045 µm, Cat. No. IPL00010) was activated with methanol for 15 seconds, then rinsed with ddH_2O for 2 mins. The membrane and one piece of filter paper were allowed to equilibrate in 1X Tris buffered saline with Tween 20 (1X TBS-T) for at least 5 minutes. Dot blots (Minifold I Dot Blot System – 10447900) were assembled as follows: one dry piece of filter paper (Whatman 1), one 1X TBST-soaked piece of filter paper, equilibrated membrane and tightly secured with the 96-well top. Typically, 50 µL samples were loaded by multichannel pipette as close to the membrane as possible. Vacuum was applied until

the liquid from the samples was passed through the membrane into the collection chamber. Wells were then rinsed with the same volume of Buffer E with vacuum. The membrane was blocked for one hour in 1X TBS-T with 1% non-fat dry milk. After addition of primary antibody (anti-SF3B1, 27684-1-AP, Proteintech, 1:7000 dilution) the membrane was incubated overnight at 4 ºC with agitation. The blots were washed three times with 1X TBS-T, followed by incubation with secondary antibody (IRDye® 680RD Donkey anti-Rabbit IgG, 926-68073, LICOR, 1:15,0000 dilution) in 1X TBS-T with 1% non-fat dry milk for 1 hour. The blots were washed three times again and imaged with the Odyssey® Infrared Imaging System (LI-COR Biosciences). Dot blot images were quantified using LICOR Image Studio Lite. Thermal unfolding data was fit to a non-linear regression, inhibitor vs. response (four parameters) curve fit in GraphPad Prism 10. Calculated IC_{50} was used as the value T_m, since the dose of temperature was increasing in lieu of drug.

Western Blot analysis

Protein samples from immunoprecipitation reactions were prepared in 5x Laemmli buffer (62.5 mM Tris, 25% glycerol, 6.25% SDS, 0.1% bromophenol blue, 5% beta-mercaptoethanol) and heated at 95ºC for 1 minute prior to loading on 10% acrylamide gels for SDS-PAGE. Gels were transferred to PVDF membrane (Immobilon FL, Bio-Rad Mini Trans-Blot Cell). Membranes were blocked{Citation} with 1% milk in 1X TRIS-buffered saline with Tween 20 (TBST) for 1 hour at room temperature while rocking. Antibody was added directly to blocking buffer and incubated overnight at 4ºC with agitation. From Proteintech: anti-SF3B1 rabbit polyclonal (27684-1-AP, used at 1:7000), SNRPB2 rabbit polyclonal (13512-1-AP, used at 1:2500). From Santa Cruz Biotech: SF3A2 mouse monoclonal (sc-390444,

used at 1:1000). After removing the primary antibody, blots were washed with 1x TBST for 5 minutes three times. Corresponding LICOR secondary antibodies: LICOR IRDye® 680RD Donkey anti-Rabbit IgG secondary antibody (P/N: 926-68073) and IRDye® 800CW Donkey anti-mouse IgG secondary antibody (P/N: 926-32212) were added at 1:15000 in 1X TBST with 1% milk and incubated at room temperature for 1 hour. After removing the secondary antibody, blots were washed with 1x TBST for 5 minutes three times. Blots were imaged with LICOR Odyssey Infrared Imager (Model #: 9120). Images were quantified using LICOR Image Studio Lite software.

Results

SF3B1 thermal stability can be measured by both western blot and dot blot analysis

To assess how SFB31 interacts with different spliceosome inhibitors in a biologically relevant context, we developed an *in vitro* thermal shift assay with HeLa nuclear extract (Fig. 2.2A). We first evaluated whether we could generate a thermal unfolding profile for SF3B1 in nuclear extract by quantifying the amount of soluble SF3B1 following heat treatment by quantitative western blot analysis. We detected a cooperative decrease in signal for ant-SF3B1 in response to increases in temperature. Analysis of the thermal denaturation curve allowed us to calculate a temperature at which half of the protein in a sample is denatured (T_m). We determined the T_m of SF3B1 in HeLa nuclear extract to be 51ºC (R^2=0.99) (Fig. 2.2B).

To overcome the challenge of screening of multiple conditions simultaneously with experimental replicates, we developed a quantitative dot blot protocol that

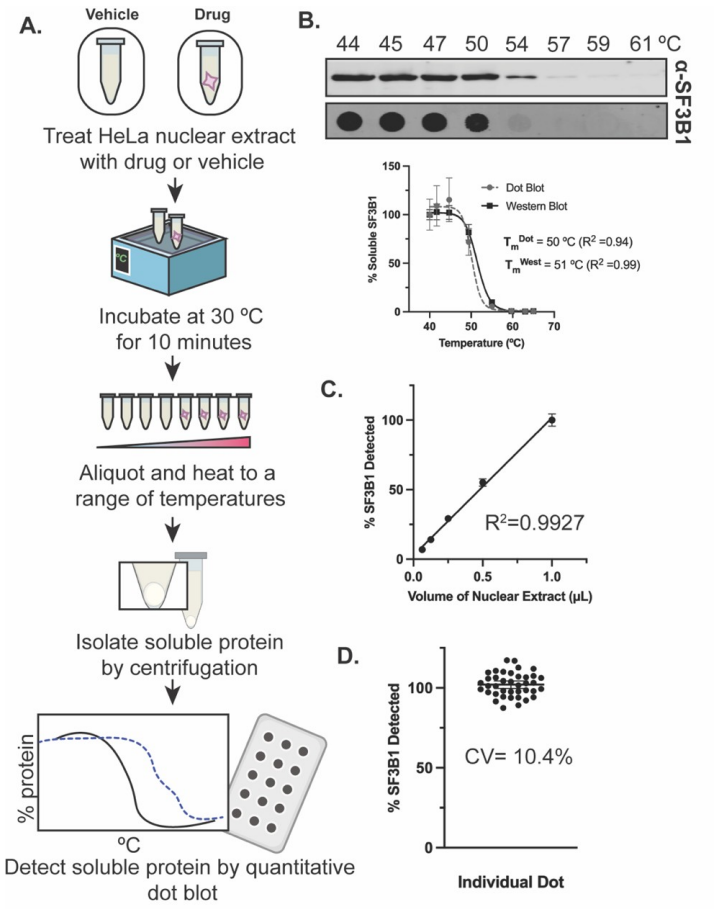

Figure 2.2. Thermal unfolding of SF3B1 is detected by western and dot blot. A) Procedural schematic of *in vitro* thermal shift assay in HeLa nuclear extract B) Western and dot blots showing SF3B1 in samples heated to temperatures shown, followed by thermal denaturation curves. Thermal shift assay was performed in triplicate. Percent soluble SF3B1 was quantified using LICOR Image Studio. An average of the signal for SF3B1 at the lowest temperature was assumed to be 100% SF3B1. C) Linear regression of anti-SF3B1 signal detected from serial dilutions of nuclear extract. Each sample was adsorbed to the dot blot in triplicate. D) Distribution of anti-SF3B1 signal when same amount of nuclear extract is adsorbed to dot blot multiple times (n=43). Average signal for n dots was used as 100% of SF3B1.

greatly increases throughput of the assay. I tested the assay's ability to accurately detect decreasing amounts of SF3B1 in a sample by analyzing serially diluted nuclear extract samples by quantitative dot blot and found that signal intensity for SF3B1 decreased linearly with decreasing nuclear extract dilution (Fig. 2.2C). I next evaluated

the precision afforded by quantitative dot blot by loading 48 identical samples. SF3B1 signal in equivalent samples exhibited a 10.4% coefficient of variation (Fig. 2.2D).

Side-by-side comparison of western and dot blot analysis produced similar thermal unfolding profiles, although, the T_m values differed slightly, with $T_m^{western}$= 51ºC (R^2=0.99) and T_m^{dot}= 50ºC (R^2=0.94) (Fig. 2.2B). With the dot blot, we find that anti-SF3B1 signal in samples subjected to non-denaturing temperatures is more variable, which influences Tm determination. We hypothesize competition associated with the increased presence of other soluble proteins in the lower temperature samples interferes with SF3B1 adsorption to a membrane. Indeed, variance of the SF3B1 signal correlates with overall protein abundance as measured by UV absorbance at 280 nm (data not shown). Western blots allowed more accurate detection of the amount of soluble SF3B1 in samples treated at lower temperatures.

Spliceostatin A shifts SF3B1 thermal stability but not pladienolide B or herboxidiene

Recent cryo-EM and crystal structures of spliceostatin A in complex with 17S U2 snRNP and purified SF3B complex respectively demonstrate that spliceostatin A arrests SF3B1 in an open conformation (Cretu et al. 2021). To determine whether the SF3B1 conformation can resist thermal denaturation in the presence of inhibitor, we heated aliquots of HeLa nuclear extract incubated with either 5 μM spliceostatin A or DMSO across a range of temperatures and used the dot blot assay to quantify the remaining soluble SF3B1. Spliceostatin A treatment induces a small but consistent increase in soluble SF3B1 abundance (Fig. 2.3A) at higher temperatures resulting in a Tm shift from 52 ºC (R^2=0.9) to 53ºC (R^2=0.9). This result supports the possibility that the inhibitor-bound open conformation of SF3B1 is more stable relative to the unbound state.

Structural models of SF3B in complex with pladienolide B (PB) and analog E7107 show the drug bound in the same tunnel that splieostatin A occupies between PHF5A and the open conformation of SF3B1 (Cretu et al. 2018, Finci et al 2018). I used the dot blot assay to test whether pladienolide. B and herboxidiene binding results in the same increase of SF3B1 thermal stability focusing on temperatures expected to capture a shift in thermal stability. Surprisingly, only nuclear extract treated with spliceostatin A and not pladienolide B or herboxidiene led to increased amounts of soluble SF3B1 at denaturing temperatures relative to DMSO (Fig. 2.3B). Despite all compounds being potent inhibitors of splicing, this result suggest spliceostatin A may induce slight differences in SF3B1 conformation compared to other compounds. The effect may also be due to spliceostatin A covalent interaction with the inhibitor binding pocket (Cretu et al., 2021). Pladienolide B does not form a covalent link with PHF5A like spliceostatin A and interacts with different residues outside of the tunnel (Cretu

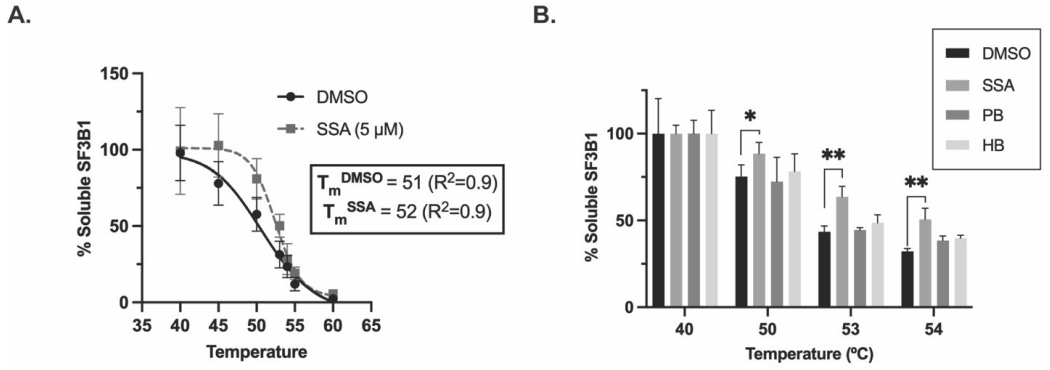

Figure 2.3. SSA shifts SF3B1 thermal stability.
A) Thermal unfolding curves of SF3B1 in HeLa nuclear extract treated with either DMSO (black circles, solid black curve) or SSA (gray squares, gray dotted line). Average signal at 40ºC was assigned as 100% anti-SF3B1 signal. B) Percent of soluble SF3B1 in samples treated with DMSO (Black), SSA (medium gray), PB (dark gray), or HB (pale gray) that were heated to temperatures near or above the Tm of untreated SF3B1. Average signal at 40ºC was assigned at 100% SF3B1.

etal., 2018, Finci et al., 2018). Herboxidiene (HB) is predicted to bind in the same manner.

SF3B1 thermal stability shows variability in different nuclear extract preparations

It is not uncommon for *in vitro* splicing and spliceosome assembly to differ across nuclear extract preps. To verify that SF3B1 thermal stability is not nuclear extract-dependent observation, we generated thermal unfolding profiles for multiple thermal stability of SF3B1 across four nuclear extract preparations. Overall, we observe no marked difference in most nuclear extract preparations the with T_m being consistently near 50ºC (Fig. 2.4A). Surprisingly, we did encounter a nuclear extract in which SF3B1 shows increased vulnerability to thermal denaturation. The T_m of 46ºC for this population of SF3B1 (Fig. 2.4B) is a pronounced difference from other nuclear extracts.

We next treated this unusual nuclear extract with spliceostatin A and generated a thermal unfolding profile. Strikingly, spliceostatin A restored the T_m of SF3B1 to that observed in the other extracts (Fig. 2.4B). We tested whether herboxidiene and pladienolide B can restore thermal stability of this unusual SF3B1 population and find that both significantly increase SF3B1 thermal stability relative to DMSO. Interestingly, we also find that an analog of herboxidiene that binds SF3B1 but does not inhibit splicing, also restores thermal stability of defective SF3B1. Based on these results, we speculate that the small increase in SF3B1 thermal stability observed following SSA-treatment of most nuclear extracts results from its presence in the 17S U2 snRNP in a stable, open conformation, while more free SF3B complex may be present in the extract with the less stable population of SF3B1. Indeed, U2 snRNA and other 17S U2 snRNP components may act as endogenous ligands of the SF3B protein subcomplex

that afford the protein conformational stability. The exogenous ligands–inhibitors may then rescue the loss in the thermal stability when SF3B1 is not associated with the snRNP.

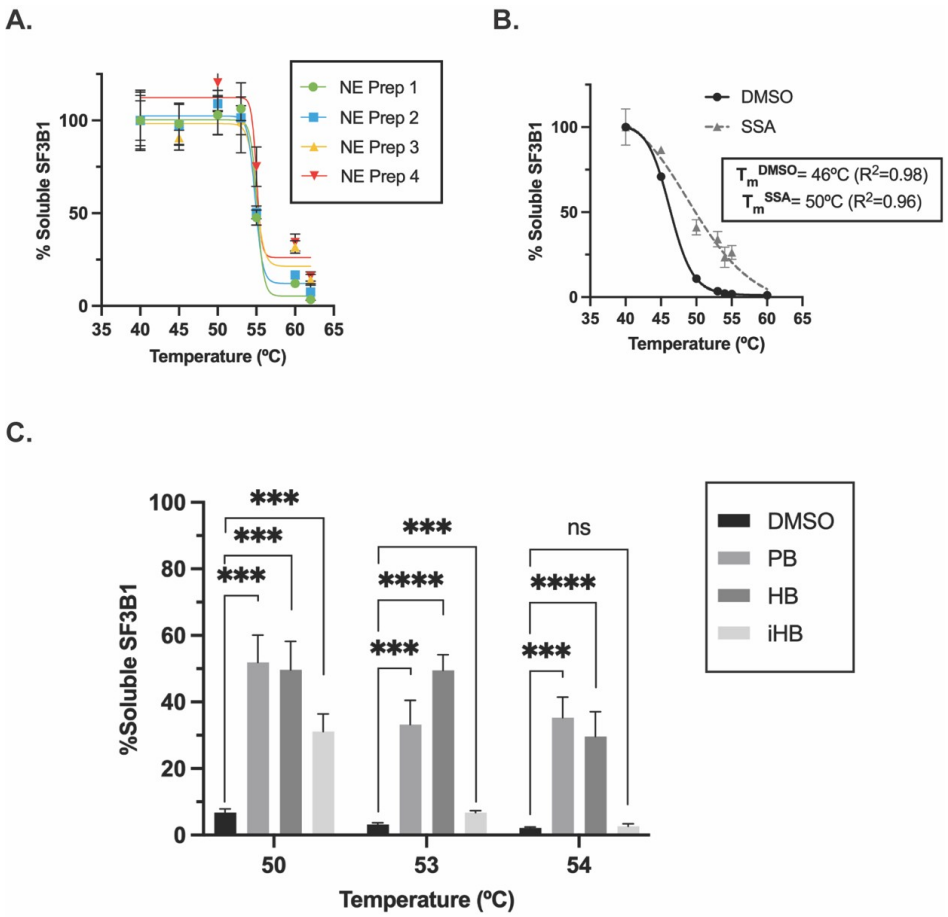

Figure 2.4. All compounds increase thermal stability in unstable SF3B1 population.
A) Thermal unfolding profiles for SF3B1 across four nuclear extract preparations. B) Thermal unfolding curves of DMSO (black) and SSA (gray) generated from a nuclear extract preparation with less thermal stable SF3B1. C) Plots of remaining soluble less stable SF3B1 at temperatures at or near the T_m of stable SF3B1 treated with DMSO, PB, HB, or iHB.

Discussion

Modulating splicing by interfering with intron selection by U2 snRNP represents a vulnerability for treating hematological cancers and suboptimal blood cell production,

as in myelodysplastic syndrome (Papaemmanuil et al., 2011, Wang et al., 2011). Screens for natural products with tumor-selective cytotoxicity led to the discovery of FR901463, GEX1 (Sakai et al., 2002), and the pladienolides (Mizui et al., 2004) with FR901463 being structurally distinct from the latter. Analogs of these natural products, spliceostatin A (FR901463) and E7107(pladienolides), with improved solubility and stability have been synthesized (Nakajima et al., 1997, Folco et al. 2011). These compounds achieve tumor suppression through splicing inhibition (Kotake et al., 2007, Yokoi et al. 2011, Effenberger et al., 2014). The ability of these compounds to diminish solid tumors cells and mouse xenografts at a low-nanomolar dose (Bonnal et al., 2012) underlines their potential as cancer therapeutics. U2 snRNP component, the heptameric SF3B complex was identified as a common pharmacophore for spliceostatin A by affinity chromatography (Kaida et al. 2007) and pladienolide B by scintillation proximity assay (Kotake et al. 2008). Analogs of potent splicing inhibitors have been generated that are unable to inhibit splicing (inactive) but compete with inhibitors to restore splicing activity (Effenberger et al. 2014). Incidentally, this supports a model where binding is insufficient to ensure inhibition. Recent structural models of 17S U2 snRNP and a drug-stalled A-like complex displays SF3B1 in an open conformation with the latter revealing mutual exclusion of the intron for bound drug (Zhang et al., 2020, Cretu et al., 2021). In contrast, structural models of complex A to B^{act} display SF3B1 in a closed conformation with the U2 snRNA/intron helix sandwiched between the N- and C- termini (Yan et al., 2016, Plaschka et al., 2018). Overall, this suggests that a potent splicing inhibitor should stabilize the open conformation of SF3B1, preventing the entry of an intron. While structural models and binding assays utilizing purified SF3B complex or 17S U2 snRNP are evidence of their

engagement with these small molecule inhibitors, this data does not necessarily capture binding in a native context.

Our group developed an assay to evaluate spliceosome inhibitor binding in nuclear extract, wherein, all accessory splicing factors are present. This assay is a modified cellular thermal shift assay (CETSA), which uses a HeLa cell-derived nuclear lysate, often used *in vitro* splicing and assembly assays, in lieu of intact cells. Thermal shift assays, which previously were restricted to purified proteins, have been adapted to reproduce the complexity of ligand binding in cells (Molina et al. 2014). Success of drugs generally relies on their ability to engage productively with one or few targets, retaining effectiveness while preventing unintended adverse effects. Remarkably, pladienolide derivatives E7107 and H3B-800 have been or are currently being evaluated for their efficacy at terminating solid tumor cells in patients (Eskens et al., 2013, Seiler et al., 2018). However, the E7107 clinical trial was aborted at phase I due to its toxicity to patients. What remains to be known about these compounds is how well they engage with SF3B in a spliceosomal context. Understanding how spliceosome targeted therapies bind in a native environment is imperative for preventing unforeseen adverse events in patients.

Our *in vitro* thermal shift assay finds that SF3B1 is amenable to thermal unfolding experiments, evidenced by a sigmoidal unfolding profile, which suggests cooperativity. I have calculated T_m values from fitting the data, which signifies the temperature at which half of the protein in a sample is denatured. This assay can also be scaled to high-throughput studies through use of quantitative dot blot, allowing replicates and multiple conditions to be assayed simultaneously on the same immunoblot. We tested spliceostatin A, herboxidiene, and pladienolide B for their

ability to shift the thermal stability of SF3B1, and detected a modest increase in SF3B1 thermal stability in spliceostatin A treated nuclear extract, but detected no change with herboxidiene or pladienolide B. Although the latter compounds comparably inhibit splicing (Kotake et al., 2007, Kaida et al., 2007, Hasegawa et al., 2011) and bind to purified SF3B complexes (Cretu et al., 2018, Cretu et al., 2021), they differ structurally from spliceostatin A. Spliceostatin A covalently modifies SF3B component, PHF5A via nucleophilic attack of the epoxide moiety by the zinc-activated thiol on cysteine 26. As mentioned previously, SF3B1 adopts an open conformation in 17S U2 snRNP prior to joining an intron to form complex A, thus without substrate to trigger closing of SF3B1, it likely remains open whether drug binds or not. This could explain why a thermal shift could not be observed for non-covalent inhibitors, pladienolide B and herboxidiene. Perhaps their binding is short-lived or reversible, whereas permanent stabilization is achieved by the drug being covalently bound to SF3B.

Different nuclear extract preparations vary in their splicing efficiency and spliceosome complex assembly in our *in vitro* splicing system, thus we wanted to assess SF3B1 thermal stability in multiple nuclear extracts. We find that SF3B1 thermally unfolds similarly across most nuclear extracts, however one nuclear extract had a population of SF3B1 that was more susceptible to thermal denaturation. Interestingly, all compounds including non-covalent inhibitors restore the thermal stability of this SF3B1 population.

Using our *in vitro* splicing assay, we tested the impact this more labile SF3B1 on splicing efficiency and found that this nuclear extract could not convert pre-mRNA to spliced product. Considering that SF3B1 participates in splicing as a component of 17S U2 snRNP and that SF3B1 in active nuclear extracts resists thermal denaturation

even in the absence of drug, we speculated that SF3B1 in the splicing-deficient nuclear extract may not be in U2 snRNP. I proposed a model that the less stable SF3B1, which does not participate in splicing maybe in its heptameric, SF3B subcomplex, but not with its stabilizing natural ligands in U2 snRNP. I found through separating spliceosome components from their complexes by glycerol gradient and subsequent fractionation that the extract with less thermal stable SF3B1 had no fractions containing both SF3B1 and U2 snRNP components. These findings suggest that binding of purified SF3B containing complexes may not capture their ability to form productive interactions with therapeutic agents in their native environment. Our thermal shift assay in HeLa nuclear extract can identify SF3B1-targeting compounds that have a sustained interaction with native SF3B1, which can be functionalized for tumor-selective splicing inhibition.

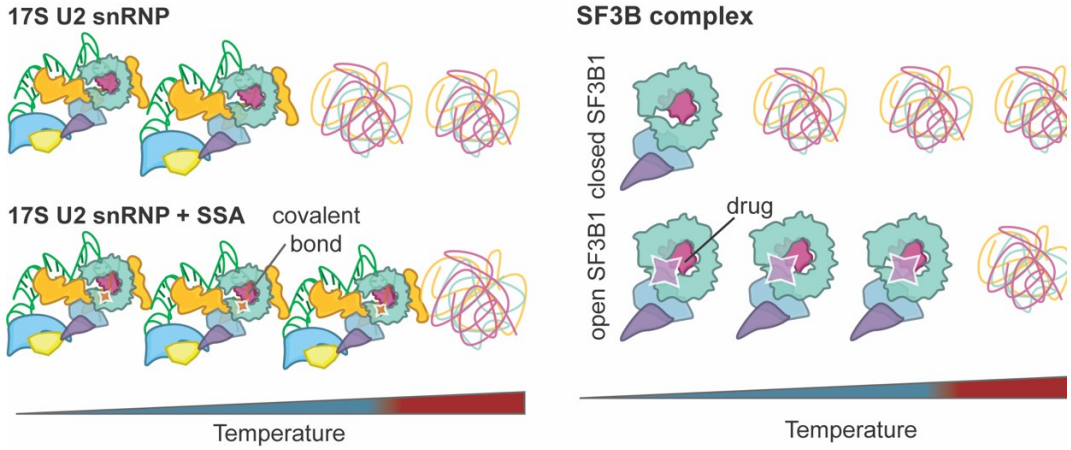

Figure 2.5. Model for SF3B thermal stability.
Schematic demonstrating model for SF3B1 thermal stability in the presence of endogenous ligand, drug, or both.

Chapter III: Reconstituting U2 snRNP interactions with an intron

Abstract

In this study, I aimed to reconstitute BPS recognition by U2 snRNP using HeLa nuclear extract with affinity tagged U2 snRNP. We speculated that U2 snRNP would require factors in the nuclear extract to not only bind introns, but also to distinguish intron from random RNA sequence. To investigate this theory, we immunoprecipitated U2 snRNP before or after incubation with minimal intron substrates and performed RNA immunoprecipitation to determine the requirements for recognition of an intron. We also tested the impact of ATP hydrolysis on intron binding and U2 snRNP protein composition. We find that U2 snRNPs isolated from nuclear extract are capable of binding minimal intron RNA with some ability to distinguish intron sequence from random RNA sequence. In addition, we learned that in the absence of ATP, U2AF is stably bound to our immunoprecipitated snRNPs and that ATP alters the protein composition of U2 snRNP.

Introduction

Splicing is catalyzed by a macromolecular machine called the spliceosome. The spliceosome assembles stepwise onto precursor mRNAs (pre-mRNAs) and is comprised of five, U-rich small nuclear RNAs and their associated proteins (snRNPs). Splicing commences with U1 snRNP and U2AF2/1 identifying the 5′ splice site (ss), polypyrimidine tract (PYT) and 3′ ss forming E complex (Will et al. 2011, Wahl et al. 2009). Initial recognition of the branch point sequence (BPS) by SF1 also occurs during the ATP-independent E complex formation (Will et al. 2002). However, selection of the branch point sequence is ultimately determined by U2 snRNP during ATP-dependent, A complex assembly. U2 snRNP identifies the branch point sequence by an unclear mechanism that is likely a cooperative process between both RNA and protein components. Long introns and inconsistent BPSs, which are typical for human genes, create equivalency among BPS candidates and suggest base-pairing between the U2 snRNA and the BPS is insufficient for accurate splicing. Previous studies show evidence that U2AF recruits U2 snRNP to a BPS through interactions with SF3B1 (Gozani et al. 1998, Cretu et al. 2016) (Fig 3.1A). Cancer-associated mutations of SF3B1 can alter 3′ ss choice, often through usage of an alternative BPS (Darman et al. 2015, DeBoever et al. 2015). These mutations are concentrated in the HEAT repeat domain of SF3B1, which cradles the 3′ end of the intron immediately prior to first step chemistry (Cretu et al. 2016, Yan et al. 2016, Carrocci et al.2018) (Fig 3.1B). Interestingly, this domain of SF3B1 is the point of contact for U2AF interactions (Cretu et al. 2016, Gozani et al. 1998), implying the importance of this protein-protein interaction and the polypyrimidine tract in identifying the ideal BPS.

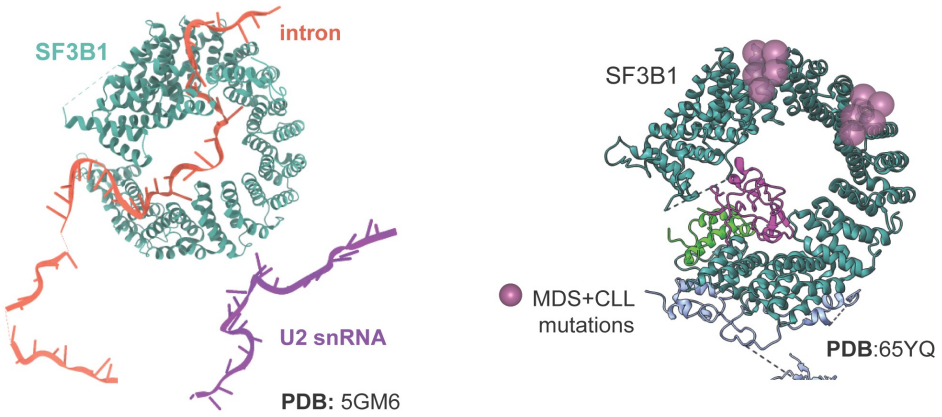

Figure 3.1. Branch point sequence selection may be influenced by polypyrimidine tract.
A) Model of yeast activated spliceosome showing the 3′ end of the intron contacting the C-terminus of SF3B1 (Yan et al. 2016). B) SF3B1 from human 17S U2 snRNP with location of MDS and chronic lymphocytic leukemia mutations depicted in magenta

Previously, Query et al. 1997 demonstrated that U2 snRNP-containing complexes that migrate similarly with A complex can be assembled in the absence of ATP on minimal introns that contain only a BPS and PYT. These minimal introns present a useful tool to study U2 snRNP interactions with an intron, especially those that are ATP-dependent, that may not be captured a full-length pre-mRNA due to their short life-span.

In this study, I reconstituted intron recognition by U2 snRNP to better understand the requirements for branch point sequence section during the ATP-driven E-to-A complex transition. Further, I assessed the impact of ATP on intron binding and U2 snRNP composition to identify events that require ATP. Here, I provide evidence for a U2 snRNP remodeling event that requires ATP hydrolysis and the minimum requirements for U2 snRNP/intron interactions.

Methods

HeLa nuclear extract

HeLa cells containing an integrated transgene for V5-tagged SNRPB2 were generated using the HILO-RMCE cassette and RMCE acceptor cells (generously provided by E. Makeyev) as described in Khandelia et al. (2011). Expression of V5-tagged SNRPB2 was induced with doxycycline 48 h prior to harvest (Kim 2019). Prior to use for the NTP studies, HeLa nuclear extract was either incubated at 30°C for 15 min to cycle residual ATP or passed through a G-50 size exclusion column to deplete residual nucleotides.

T7 run-off transcription

For minimal introns used in binding assays, DNA oligonucleotides containing a T7 promoter sequence and the appropriate minimal in intron sequence were annealed and used as templates using standard T7 run-off transcription reactions including G(5′) ppp(5′)G cap analog (New England Biolabs) and ^{32}Pα-UTP. Transcripts were purified by G-25 resin size exclusion (Sephadex, 9041-35-4).

Immunoprecipitation/ RNA Immunoprecipitation

Prior to immunoprecipitation experiments HeLa nuclear extract generated from cells expressing V5-SNRPB2 was diluted to 60% (v/v) with a buffer containing 2 mM magnesium acetate, 20 mM potassium glutamate, and either 2 mM ATP, GTP, AMP-PnP or nuclease-free water. For in-extract binding experiments, either 60 nM of radiolabeled synthetic intron or an equivalent volume of nuclease-free water were added to the nuclear extract preparation and incubated at 30 ºC for 10 minutes. Nuclear extract preparations incubated with 2-5 µg of mouse anti-V5 (GenScript A01724-100, Invitrogen R960-25) overnight at 4 ºC rotating end over end. Protein A

magnetic bead (New England Biolabs S1425S) aliquots of 20 µL washed with 1X PBS were then incubated with anti-V5 treated nuclear extract for 4 hours at 4 ºC while rotating. The beads were washed 3 times with IP wash buffer (20 mM Tris pH 7.9, 120 mM KCl, 1 mM EGTA, 0.1% NP-40, 5% glycerol) and complexes were eluted either with 0.1 M Glycine pH 2.5 for protein analysis or with 100 mM Tris pH 7.5, 10 mM EDTA, 1% SDS, 150 mM sodium chloride, 0.3 M sodium acetate pH 4.8 for RNA analysis. For RNA analysis, elutions were spiked with a known concentration of a 398 nt radiolabeled RNA to control for precipitation efficiency. The elution were then subjected to 25:24:1 phenol:chloroform:isoamyl alcohol extraction and ethanol precipitation of the aqueous layer. Aliquots of input and flow-through were prepared in the same way.

For isolated U2 snRNP binding, the same procedure was used except that intron was omitted prior to addition of magnetic beads. Instead, radiolabeled 60 nM intron in IP wash buffer was added to beads after washing and incubated for 90 minutes at 4 ºC with rotation. The beads were then washed again 3 times with IP wash buffer before elution.

Western Blot analysis

Protein samples from immunoprecipitation reactions were prepared in 5x Laemmli buffer (62.5 mM Tris, 25% glycerol, 6.25% SDS, 0.1% bromophenol blue, 5% beta-mercaptoethanol) and heated at 95ºC for 1 minute prior to loading on 10% acrylamide gels for SDS-PAGE. Gels were transferred to PVDF membrane (Immobilon FL, Bio-Rad Mini Trans-Blot Cell). Membranes were blocked with 1% milk in 1X TRIS-buffered saline with Tween 20 (TBST) for 1 hour at room temperature while rocking. Antibody was added directly to blocking buffer and incubated overnight at 4ºC

with agitation. From Proteintech: anti-DHX15 rabbit polyclonal (12265-1-AP, used at 1:1000), SNRPB2 rabbit polyclonal (13512-1-AP, used at 1:2500), and U2AF1 mouse monoclonal (60289-1-Ig, used at 1:1000). From Santa Cruz Biotech: SF3A2 mouse monoclonal (sc-390444, used at 1:1000). After removing the primary antibody, blots were washed with 1x TBST for 5 minutes three times. Corresponding LICOR secondary antibodies: LICOR IRDye® 680RD Donkey anti-Rabbit IgG secondary antibody (P/N: 926-68073) and IRDye® 800CW Donkey anti-mouse IgG secondary antibody (P/N: 926-32212) were added at 1:15000 in 1X TBST with 1% milk and incubated at room temperature for 1 hour. After removing the secondary antibody, blots were washed with 1x TBST for 5 minutes three times. Blots were imaged with the LICOR Odyssey Infrared Imager (Model #: 9120). Images were quantified using LICOR Image Studio Lite software.

RNA denaturing gel analysis

Precipitated RNA was resuspended in FEB (95% formamide, 20 mM EDTA, 0.01% bromophenol blue and 0.01% cyan blue) and separated by 15% urea-PAGE. Gels were dried onto filter paper and visualized by phosphorimaging. Images were quantified using FIJI software (Image J).

Results

U2 snRNP isolated from nuclear extract can bind intron RNA

We developed a HeLa nuclear extract with V5-tagged SNRPB2 (Khandelia et al. 2011, Maul-Newby et al. 2022), a core U2 snRNP protein (Fig 3.3B). This tool allows us the pull the entire snRNP out of nuclear extract and co-elute its binding partners. We speculated that U2 snRNP requires factors present in nuclear extract to stably

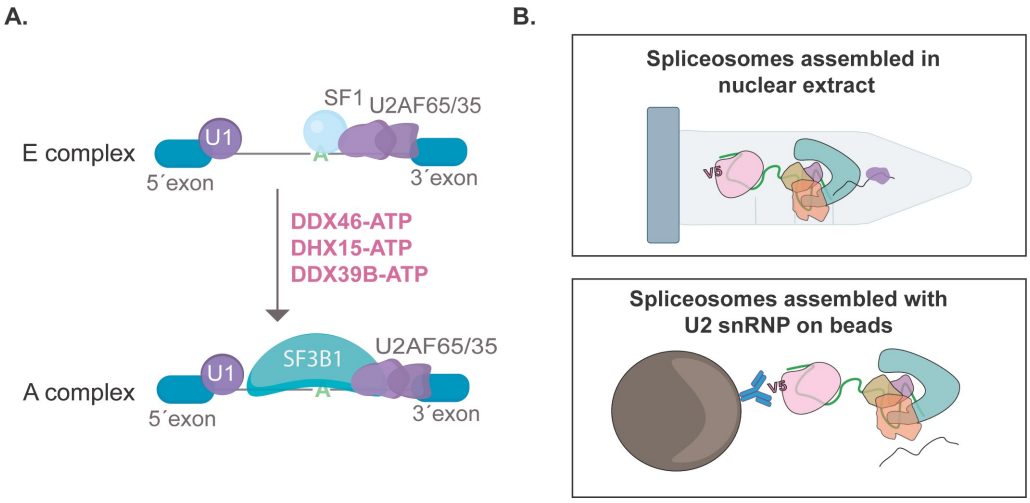

Figure 3.2. Requirements for U2 snRNP-intron interaction
A) Schematic adapted from Gozani et al. 1998, showing model for U2 snRNP recruitment to the branch point sequence by U2AF65 during E to A complex transition. B) Schematic of U2 snRNP binding assay conditions.

associate with an intron (Fig 3.2A). This hypothesis predicts that U2 snRNP from isolated from nuclear extract will not bind a pre-mRNA, while U2 snRNP in nuclear extract will bind. I considered that use of a full-length pre-mRNA to test this prediction may result in the co-immunoprecipitation of splicing intermediates or mRNA, not necessarily capturing intron recognition events. Instead, I decided to use a minimal intron substrate. Query et al. 1997 previously demonstrated that in the absence of ATP, a A-like complex can be assembled on an RNA with only a branch point sequence (BPS) and polypyrimidine tract (PYT). This non-canonical substrate is incapable of being spliced and thus is only capable of early U2 snRNP binding events.

For my experiments, I added an intron RNA with the consensus BPS and U2AF2 binding motif of multiple U's occasionally interrupted a C for the PYT (BPS-PYT) (Agrawal et al. 2016) or a scrambled sequence (Fig. 3.3A) to either to nuclear extract or immunoprecipitated U2 snRNP followed by RNA immunoprecipitation (IP). I

analyzed the co-immunoprecipitated RNA by denaturing Urea PAGE to quantify input and elutions (Fig 3.3B). As expected, when BPS-PYT RNA was added to nuclear extract, it co-eluted with U2 snRNP suggesting that this RNA stably engages with the snRNP in nuclear extract. Surprisingly, BPS-PYT RNA incubated with beads attached to U2 snRNP isolated from nuclear extract, still co-eluted with U2 snRNP. My evidence

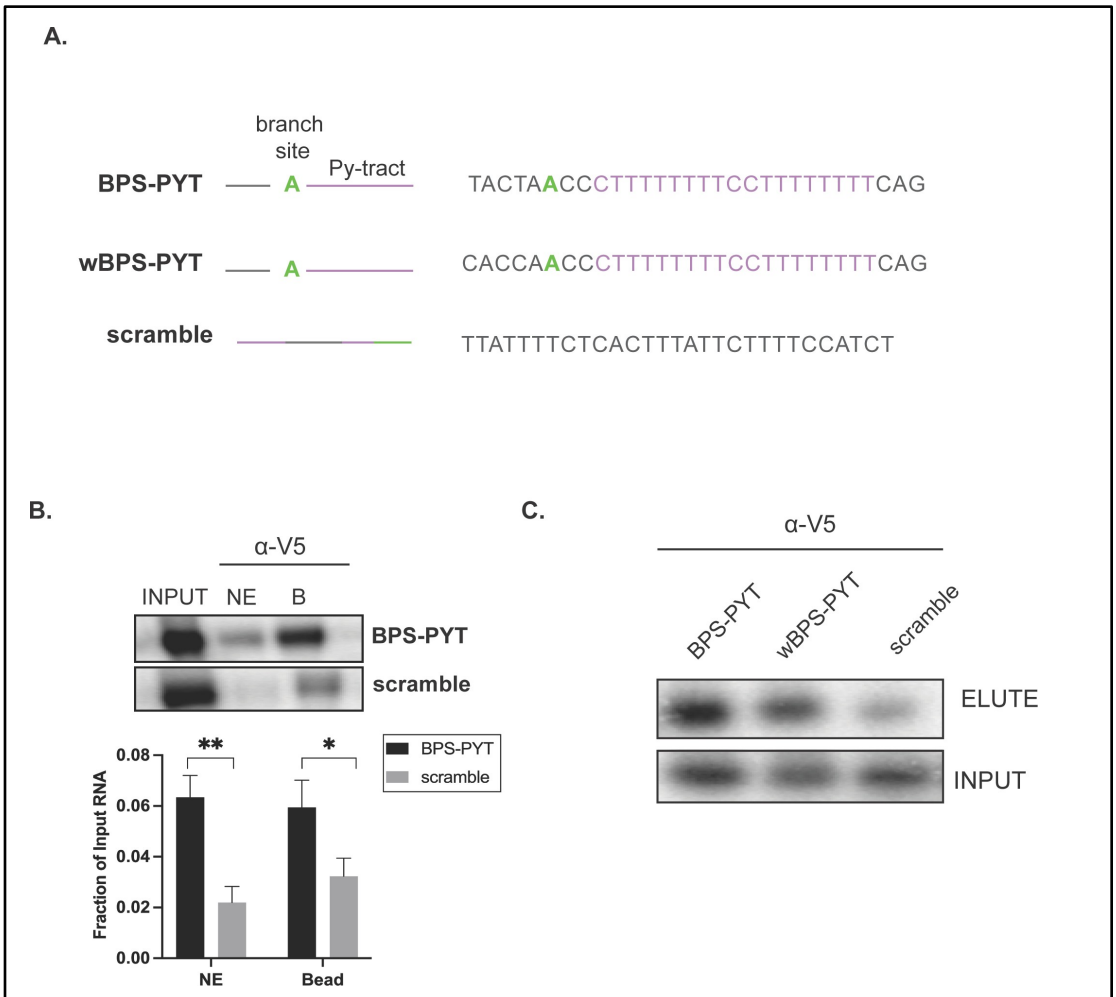

Figure 3.3 BPS-PYT RNA binds U2 snRNP on beads.
A) Sequences of different RNAs used in U2 snRNP binding experiments B) Denaturing gel showing RNA immunoprecipitated from spliceosome complexes assembled in nuclear extract (NE) or from U2 snRNP complexes assembled with immunoprecipitated snRNPs (B for bead) and quantification of fraction of input remaining in eluted RNA. C) Same as B), but only RNA eluted U2 snRNP complexes assembled on beads is shown.

points to two possible scenarios, either the immunoprecipitated U2 snRNP is still bound to factors that aid in BPS-PYT binding, or additional factors are not required for intron binding. The scrambled RNA co-eluted with U2 snRNP in both contexts to a significantly lesser extent, suggesting that the interaction between the snRNP and intron is sequence specific.

U2 snRNP isolated from nuclear extract can bind mutated intron RNA

Although human branch point sequences have a general formula of yUnAy (Gao et al. 2008), they are not conserved, giving rise to degenerate BPS candidates. Cancer-associated mutations in SF3B1 can lead to erroneous BPS selection, producing aberrant transcripts even with canonical 3′ splice site (ss) usage (Darman et al. 2015). Splicing in humans requires flexibility to accommodate divergent BPSs, while maintaining accuracy in the selection process. In addition to 5′ and 3′ splice sites, another intron landmark, the polypyrimidine tract can influence splicing fidelity (Reed et al. 1989, Coolidge et al. 1997). We hypothesized that the quality of the polypyrimidine tract (PYT) can counteract an imperfect BPS or disqualify a consensus BPS through interactions with regulatory factors within the nuclear extract. Conversely, we speculated that introns with a weak BPS may be unable to bind U2 snRNP isolated from nuclear extract even with a compensatory high-quality PYT. To assess the influence of BPS and PYT sequence on BPS choice, we measured the ability of immunoprecipitated U2 snRNP to bind minimal intron RNAs with either a strong BPS and weak PYT (BPS-sc) or a weak BPS and strong PYT (wBPS-PYT) (Fig. 3.3A-B). I found that both BPS-sc and wBPS-PYT co-elute with U2 snRNP isolated from nuclear extract (Fig. 3.3C). This result could indicate that the polypyrimidine tract strength can minimize the effect of a weak branch point sequence on intron recognition. However,

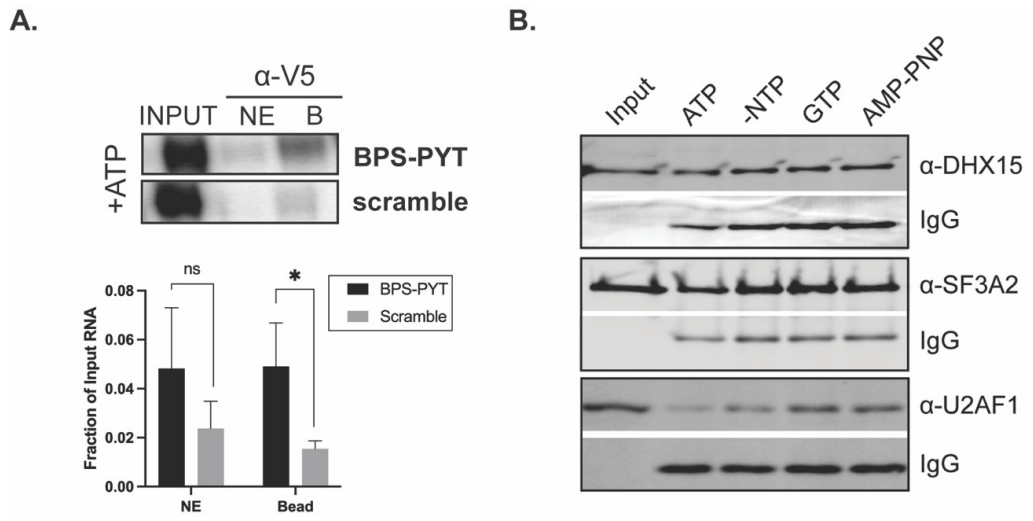

Figure 3.4 ATP alters protein composition of U2 snRNP.
A) Denaturing gel showing RNA immunoprecipitated from spliceosome complexes following ATP-treatment of nuclear extract (NE). U2 snRNP on beads (B) was immunoprecipitated from nuclear extract that was treated with ATP. B) Western blot analysis of protein composition of immunoprecipitated U2 snRNP following treatment of nuclear extract with ATP, GTP, AMP-PNP or untreated.

the possibility that this is due to the human U2 snRNP being more permissive to suboptimal branch point sequences.

U2 snRNP does not require U2AF to bind BPS-PYT RNA

Splicing factor, U2AF has previously been shown to recruit U2 snRNP to an intron through interactions with SF3B1 (Gozani et al. 1998). Given that isolated U2 snRNP was able to bind BPS-PYT RNA, we wanted to test whether U2AF was bound to the snRNP. Our western blot determined that U2AF co-elutes with IPed U2 snRNP, thus its requirement for U2/intron interactions cannot be ruled out. This suggests that U2AF is stably bound to U2 snRNP likely via interactions with SF3B1 as previously demonstrated (Gozani et al. 1998, Cretu et al. 2016). The transition from E to A complex requires ATP hydrolysis for presently uncharacterized structural rearrangements suggested by comparison of the 17S U2 snRNP (Zhang et al. 2020) and prespliceosome structural models (Plashka et al. 2018). U2AF association with

SF3B1 is less stable than in E complex (Gozani et al. 1998) and is not present in prespliceosome structural models, thus it is possible that one ATP-dependent event could be the hand-off of PYT from U2AF2 to SFB31. The later B^{act} complex (Yan et al. 2016, Carrocci et al. 2018) reveals that the C-terminus of SF3B1 cradles the PYT in lieu of U2AF2 in E complex. We suspected that U2AF heterodimer would be required for U2 snRNP/intron engagement, and that its departure from the spliceosome may be one such ATP-dependent rearrangement. To test the possibility that the departure of U2AF from U2 snRNP is one of the ATP-dependent events leading in the E to A complex transition, promoting BPS selection, we treated nuclear extract with ATP prior to immunoprecipitation of U2 snRNP and used western blot to detect the presence of U2AF. U2AF does co-elute with U2 snRNP isolated from ATP-treated nuclear extract (Fig. 3.4B), but to a much lesser extent suggesting that U2AF removal could be one of the aforementioned structural rearrangements. ATP-dependent spliceosome dynamics are driven by RNA-dependent helicases, most of which have a DEAD (DDX) or DEAH (DHX) motif. DDX and DHX enzymes differ in their selectivity of NTP energy source (O'Day et al. 1996; Uhlmann-Schiffler et al. 2006; Shen et al. 2007). DDX enzymes are limited to ATP as an energy source for activity, whereas DHX enzymes can use other NTPs with preference for purines (Robert-Paganin et al. 2017). Destabilization of U2AF from U2 snRNP is not recapitulated in nuclear extract treated with GTP or AMP-PNP, a slowly hydrolyzed ATP analog, evident of DDX activity requiring ATP hydrolysis.

ATP-treatment did not affect binding of the isolated snRNP to BPS-PYT RNA or scrambled control (Fig 3.3A). Given our previous result that ATP-treatment reduces

U2AF association with U2 snRNP, I conclude that U2AF is may be inessential for binding of BPS-PYT RNA to isolated U2 snRNP.

Discussion

U2 snRNP defines the boundaries of an intron through identification of the branch point sequence and subsequent 3′ splice site selection. Although the spliceosome makes initial contact with the branch point sequence through SF1 (Liu et al. 2001), this process is passive and does not necessarily commit a pre-mRNA to splicing. Spliced products are determined during the E to A complex transition when U2 snRNP establishes the intron-exon boundaries through its dynamic, ATP-dependent selection of the branch point sequence. Branch point sequences are poorly conserved in human genes, suggesting base-pairing between the U2 snRNA and intron is insufficient to ensure splicing fidelity. To better understand the minimum requirements for intron recognition by U2 snRNP, I aimed to reconstitute this event in the absence of extraneous splicing factors by incubating immunoprecipitated U2 snRNP with a minimal intron RNA. Interestingly, the minimal intron RNA, and the scrambled control–to a significantly lesser extent, co-elute with the isolated U2 snRNP. This evidence suggested that the immunoprecipitated U2 snRNP either did not require splicing factors to bind RNA in a sequence dependent manner, or that I had not isolated U2 snRNP from these factors. Western analysis of immunoprecipitated U2 snRNP revealed that U2AF, a splicing factor that recruits U2 snRNP to introns (Gozani et al., 1998), co-elutes with U2 snRNP. This finding could suggest that U2AF is stably associated with U2 snRNP until intron recognition is achieved. Inspection of recent CryoEM models of 17S U2 snRNP (Zhang et al. 2020) and A (Plaschka et al. 2018)

and B^{act} complexes (Yan et al. 2016) indicates that U2 snRNP will experience many structural rearrangements, which likely require ATP. Notably, U2AF is not present in the A complex structure, and in the later B^{act} complex (Yan et al. 2016) SF3B1 takes hold of the 3′ end of the intron, so I speculated that U2AF departure maybe an ATP-dependent step. To test this theory, I immunoprecipitated U2 snRNP from ATP-treated nuclear extract and have identified destabilization of the U2AF heterodimer from U2 snRNP as a probable ATP-dependent remodeling events in the E-to-A complex transition. Further, I find that immunoprecipitated U2 snRNP co-elutes U2AF following GTP, slowly cleaved ATP, and no NTP treatment. Dissociation of U2AF from U2 snRNP is only achieved by ATP-treatment. The NTP-dependent structural rearrangements throughout the splicing cycle are driven by RNA-dependent NTPases, which either have a DEAH (DHX) or DEAD-box (DDX) motif. DHX and DDX enzymes both prefer to utilize ATP to drive their activity. However, DDX enzymes can only operate using ATP (Hilbert et al. 2009, Gilman et al. 2017) while DHX enzymes can use other NTPs (Robert-Paganin et al. 2017), with preference for purines. I conclude that the U2AF/SF3B1 interaction is likely destabilized through the activity of A complex DDX enzymes, DDX46 and DDX39B. U2AF was not depleted completely following ATP-treatment, which could indicate that I either do not have U2 snRNP in an A-like complex, or that U2AF does not leave the spliceosome until later steps. Interaction between U2AF and DDX39B were demonstrated biochemically (Fleckner et al. 1997) supporting a model for U2AF recruiting the helicase to a pre-mRNA. In contrast, DDX46 appears in the 17S U2 snRNP structure and whether it is involved in this rearrangement cannot be ruled out. Next, I tested the ability of ATP-treated U2 snRNP to bind to minimal intron RNA to determine whether U2AF was required for sequence-

specific intron recognition. I found that U2 snRNP isolated from ATP-treated nuclear extract co-elutes the minimal intron RNA and significantly more efficiently than scrambled control. This evidence suggests that U2AF could be indispensable for this binding event, but a more complete depletion is necessary to confirm this finding. What remains unclear is whether U2 snRNP fully depleted of U2AF can bind a minimal intron, which could be achieved using poly-U Sepharose (Zamore and Green, 1991). Isolation of native complexes would be helpful for confirming whether the events I observed were attributed to E complex or A complex spliceosomes. Mass spectrometry analysis revealed that these complexes were more heterogenous than anticipated, several non-splicing factors were identified, which complicates interpretation of the results substantially. Lastly, identifying the ATP-dependent steps that precede branch point sequence selection, and assigning these steps to activity of a particular helicase would advance our mechanistic understanding of canonical splicing.

References

Agrawal, A. A., Salsi, E., Chatrikhi, R., Henderson, S., Jenkins, J. L., Green, M. R., Ermolenko, D. N., & Kielkopf, C. L. (2016). An extended U2AF(65)-RNA-binding domain recognizes the 3' splice site signal. Nature communications, 7, 10950. https://doi.org/10.1038/ncomms10950

Alsafadi, S., Houy, A., Battistella, A., Popova, T., Wassef, M., Henry, E., Tirode, F., Constantinou, A., Piperno-Neumann, S., Roman-Roman, S., Dutertre, M., & Stern, M. H. (2016). Cancer-associated SF3B1 mutations affect alternative splicing by promoting alternative branchpoint usage. Nature communications, 7, 10615. https://doi.org/10.1038/ncomms10615

Behrens, S. E., Tyc, K., Kastner, B., Reichelt, J., & Lührmann, R. (1993). Small nuclear ribonucleoprotein (RNP) U2 contains numerous additional proteins and has a bipartite RNP structure under splicing conditions. Molecular and cellular biology, 13(1), 307–319. https://doi.org/10.1128/mcb.13.1.307-319.1993

Behzadnia, N., Hartmuth, K., Will, C. L., & Lührmann, R. (2006). Functional spliceosomal A complexes can be assembled in vitro in the absence of a penta-snRNP. RNA (New York, N.Y.), 12(9), 1738–1746. https://doi.org/10.1261/rna.120606

Berget, S. M., Moore, C., & Sharp, P. A. (1977). Spliced segments at the 5′ terminus of adenovirus 2 late mRNA. Proceedings of the National Academy of Sciences, 74(8), 3171–3175. https://doi.org/10.1073/pnas.74.8.3171

Bonnal, S., Vigevani, L., & Valcárcel, J. (2012). The spliceosome as a target of novel antitumour drugs. Nature reviews. Drug discovery, 11(11), 847–859. https://doi.org/10.1038/nrd3823

Burge, C. B., Padgett, R. A., & Sharp, P. A. (1998). Evolutionary fates and origins of U12-type introns. Molecular cell, 2(6), 773–785. https://doi.org/10.1016/s1097-2765(00)80292-0

Carrocci, T. J., Paulson, J. C., & Hoskins, A. A. (2018). Functional analysis of Hsh155/SF3b1 interactions with the U2 snRNA/branch site duplex. RNA (New York, N.Y.), 24(8), 1028–1040. https://doi.org/10.1261/rna.065664.118

Chow, L. T., Gelinas, R. E., Broker, T. R., & Roberts, R. J. (1977). An amazing sequence arrangement at the 5′ ends of adenovirus 2 messenger RNA. Cell, 12(1), 1–8. https://doi.org/10.1016/0092-8674(77)90180-5

Colgan, D. F., & Manley, J. L. (1997). Mechanism and regulation of mRNA polyadenylation. Genes & development, 11(21), 2755–2766. https://doi.org/10.1101/gad.11.21.2755

Coolidge, C. J., Seely, R. J., & Patton, J. G. (1997). Functional analysis of the polypyrimidine tract in pre-mRNA splicing. Nucleic acids research, 25(4), 888–896. https://doi.org/10.1093/nar/25.4.888

Corrionero, A., Miñana, B., & Valcárcel, J. (2011). Reduced fidelity of branch point recognition and alternative splicing induced by the anti-tumor drug spliceostatin A. Genes & development, 25(5), 445–459. https://doi.org/10.1101/gad.2014311

Cretu, C., Agrawal, A. A., Cook, A., Will, C. L., Fekkes, P., Smith, P. G., Lührmann, R., Larsen, N., Buonamici, S., & Pena, V. (2018). Structural Basis of Splicing Modulation by Antitumor Macrolide Compounds. Molecular cell, 70(2), 265–273.e8. https://doi.org/10.1016/j.molcel.2018.03.011

Cretu, C., Gee, P., Liu, X., Agrawal, A., Nguyen, T. V., Ghosh, A. K., Cook, A., Jurica, M., Larsen, N. A., & Pena, V. (2021). Structural basis of intron selection by U2 snRNP in the presence of covalent inhibitors. Nature communications, 12(1), 4491. https://doi.org/10.1038/s41467-021-24741-1

Cretu, C., Schmitzová, J., Ponce-Salvatierra, A., Dybkov, O., De Laurentiis, E. I., Sharma, K., Will, C. L., Urlaub, H., Lührmann, R., & Pena, V. (2016). Molecular Architecture of SF3b and Structural Consequences of Its Cancer-Related Mutations. Molecular cell, 64(2), 307–319. https://doi.org/10.1016/j.molcel.2016.08.036

Darman, R. B., Seiler, M., Agrawal, A. A., Lim, K. H., Peng, S., Aird, D., Bailey, S. L., Bhavsar, E. B., Chan, B., Colla, S., Corson, L., Feala, J., Fekkes, P., Ichikawa, K., Keaney, G. F., Lee, L., Kumar, P., Kunii, K., MacKenzie, C., Matijevic, M., … Buonamici, S. (2015). Cancer-Associated SF3B1 Hotspot Mutations Induce Cryptic 3' Splice Site Selection through Use of a Different Branch Point. Cell reports, 13(5), 1033–1045. https://doi.org/10.1016/j.celrep.2015.09.053

DeBoever, C., Ghia, E. M., Shepard, P. J., Rassenti, L., Barrett, C. L., Jepsen, K., Jamieson, C. H., Carson, D., Kipps, T. J., & Frazer, K. A. (2015). Transcriptome sequencing reveals potential mechanism of cryptic 3' splice site selection in SF3B1-mutated cancers. PLoS computational biology, 11(3), e1004105. https://doi.org/10.1371/journal.pcbi.1004105

De Kesel, J., Fijalkowski, I., Taylor, J., & Ntziachristos, P. (2022). Splicing dysregulation in human hematologic malignancies: beyond splicing mutations. Trends in immunology, 43(8), 674–686. https://doi.org/10.1016/j.it.2022.06.006

Dignam, J. D., Lebovitz, R. M., & Roeder, R. G. (1983). Accurate transcription initiation by RNA polymerase II in a soluble extract from isolated mammalian nuclei. Nucleic acids research, 11(5), 1475–1489. https://doi.org/10.1093/nar/11.5.1475

Effenberger, K. A., Anderson, D. D., Bray, W. M., Prichard, B. E., Ma, N., Adams, M. S., Ghosh, A. K., & Jurica, M. S. (2014). Coherence between cellular responses and in vitro splicing inhibition for the anti-tumor drug pladienolide B and its analogs. The Journal of biological chemistry, 289(4), 1938–1947. https://doi.org/10.1074/jbc.M113.515536

Effenberger, K. A., Urabe, V. K., Prichard, B. E., Ghosh, A. K., & Jurica, M. S. (2016). Interchangeable SF3B1 inhibitors interfere with pre-mRNA splicing at multiple stages. RNA (New York, N.Y.), 22(3), 350–359. https://doi.org/10.1261/rna.053108.115

Eskens, F. A., Ramos, F. J., Burger, H., O'Brien, J. P., Piera, A., de Jonge, M. J., Mizui, Y., Wiemer, E. A., Carreras, M. J., Baselga, J., & Tabernero, J. (2013). Phase I pharmacokinetic and pharmacodynamic study of the first-in-class spliceosome inhibitor E7107 in patients with advanced solid tumors. Clinical cancer research : an official journal of the American Association for Cancer Research, 19(22), 6296–6304. https://doi.org/10.1158/1078-0432.CCR-13-0485

Fica, S. M., Tuttle, N., Novak, T., Li, N. S., Lu, J., Koodathingal, P., Dai, Q., Staley, J. P., & Piccirilli, J. A. (2013). RNA catalyses nuclear pre-mRNA splicing. Nature, 503(7475), 229–234. https://doi.org/10.1038/nature12734

Finci, L. I., Zhang, X., Huang, X., Zhou, Q., Tsai, J., Teng, T., Agrawal, A., Chan, B., Irwin, S., Karr, C., Cook, A., Zhu, P., Reynolds, D., Smith, P. G., Fekkes, P., Buonamici, S., & Larsen, N. A. (2018). The cryo-EM structure of the SF3b spliceosome

complex bound to a splicing modulator reveals a pre-mRNA substrate competitive mechanism of action. Genes & development, 32(3-4), 309–320. https://doi.org/10.1101/gad.311043.117

Fleckner, J., Zhang, M., Valcárcel, J., & Green, M. R. (1997). U2AF65 recruits a novel human DEAD box protein required for the U2 snRNP-branchpoint interaction. Genes & development, 11(14), 1864–1872. https://doi.org/10.1101/gad.11.14.1864

Folco, E. G., Coil, K. E., & Reed, R. (2011). The anti-tumor drug E7107 reveals an essential role for SF3b in remodeling U2 snRNP to expose the branch point-binding region. Genes & development, 25(5), 440–444. https://doi.org/10.1101/gad.2009411

Gamboa Lopez, A., Allu, S. R., Mendez, P., Chandrashekar Reddy, G., Maul-Newby, H. M., Ghosh, A. K., & Jurica, M. S. (2021). Herboxidiene Features That Mediate Conformation-Dependent SF3B1 Interactions to Inhibit Splicing. ACS chemical biology, 16(3), 520–528. https://doi.org/10.1021/acschembio.0c00965

Gao, K., Masuda, A., Matsuura, T., & Ohno, K. (2008). Human branch point consensus sequence is yUnAy. Nucleic acids research, 36(7), 2257–2267. https://doi.org/10.1093/nar/gkn073

Gilman, B., Tijerina, P., & Russell, R. (2017). Distinct RNA-unwinding mechanisms of DEAD-box and DEAH-box RNA helicase proteins in remodeling structured RNAs and RNPs. Biochemical Society transactions, 45(6), 1313–1321. https://doi.org/10.1042/BST20170095

Gozani, O., Potashkin, J., & Reed, R. (1998). A potential role for U2AF-SAP 155 interactions in recruiting U2 snRNP to the branch site. Molecular and cellular biology, 18(8), 4752–4760. https://doi.org/10.1128/MCB.18.8.4752

Hasegawa, M., Miura, T., Kuzuya, K., Inoue, A., Won Ki, S., Horinouchi, S., Yoshida, T., Kunoh, T., Koseki, K., Mino, K., Sasaki, R., Yoshida, M., & Mizukami, T. (2011). Identification of SAP155 as the target of GEX1A (Herboxidiene), an antitumor natural product. ACS chemical biology, 6(3), 229–233. https://doi.org/10.1021/cb100248e

Hilbert, M., Karow, A. R., & Klostermeier, D. (2009). The mechanism of ATP-dependent RNA unwinding by DEAD box proteins. Biological chemistry, 390(12), 1237–1250. https://doi.org/10.1515/BC.2009.135

Hsu, T. Y., Simon, L. M., Neill, N. J., Marcotte, R., Sayad, A., Bland, C. S., Echeverria, G. V., Sun, T., Kurley, S. J., Tyagi, S., Karlin, K. L., Dominguez-Vidaña, R., Hartman, J. D., Renwick, A., Scorsone, K., Bernardi, R. J., Skinner, S. O., Jain, A., Orellana, M., Lagisetti, C., … Westbrook, T. F. (2015). The spliceosome is a therapeutic vulnerability in MYC-driven cancer. Nature, 525(7569), 384–388. https://doi.org/10.1038/nature14985

Jafari, R., Almqvist, H., Axelsson, H., Ignatushchenko, M., Lundbäck, T., Nordlund, P., & Martinez Molina, D. (2014). The cellular thermal shift assay for evaluating drug target interactions in cells. Nature protocols, 9(9), 2100–2122. https://doi.org/10.1038/nprot.2014.138

Kaida, D., Motoyoshi, H., Tashiro, E., Nojima, T., Hagiwara, M., Ishigami, K., Watanabe, H., Kitahara, T., Yoshida, T., Nakajima, H., Tani, T., Horinouchi, S., & Yoshida, M. (2007). Spliceostatin A targets SF3b and inhibits both splicing and nuclear retention of pre-mRNA. Nature chemical biology, 3(9), 576–583. https://doi.org/10.1038/nchembio.2007.18

Khandelia, P., Yap, K., & Makeyev, E. V. (2011). Streamlined platform for short hairpin RNA interference and transgenesis in cultured mammalian cells. Proceedings of the National Academy of Sciences of the United States of America, 108(31), 12799–12804. https://doi.org/10.1073/pnas.1103532108

Kotake, Y., Sagane, K., Owa, T., Mimori-Kiyosue, Y., Shimizu, H., Uesugi, M., Ishihama, Y., Iwata, M., & Mizui, Y. (2007). Splicing factor SF3b as a target of the antitumor natural product pladienolide. Nature chemical biology, 3(9), 570–575. https://doi.org/10.1038/nchembio.2007.16

Krämer A. (1996). The structure and function of proteins involved in mammalian pre-mRNA splicing. Annual review of biochemistry, 65, 367–409. https://doi.org/10.1146/annurev.bi.65.070196.002055

Langford, C. J., & Gallwitz, D. (1983). Evidence for an intron-contained sequence required for the splicing of yeast RNA polymerase II transcripts. Cell, 33(2), 519–527. https://doi.org/10.1016/0092-8674(83)90433-6

Lee, Y., & Rio, D. C. (2015). Mechanisms and Regulation of Alternative Pre-mRNA Splicing. Annual review of biochemistry, 84, 291–323. https://doi.org/10.1146/annurev-biochem-060614-034316

Lee, SW., Abdel-Wahab, O. Therapeutic targeting of splicing in cancer. Nat Med 22, 976–986 (2016). https://doi.org/10.1038/nm.4165

Lerner, M., Boyle, J., Mount, S. et al. Are snRNPs involved in splicing?. Nature 283, 220–224 (1980). https://doi.org/10.1038/283220a0

Liu, Z., Luyten, I., Bottomley, M. J., Messias, A. C., Houngninou-Molango, S., Sprangers, R., Zanier, K., Krämer, A., & Sattler, M. (2001). Structural basis for recognition of the intron branch site RNA by splicing factor 1. Science (New York, N.Y.), 294(5544), 1098–1102. https://doi.org/10.1126/science.1064719

Liu, Z., Yoshimi, A., Wang, J., Cho, H., Chun-Wei Lee, S., Ki, M., Bitner, L., Chu, T., Shah, H., Liu, B., Mato, A. R., Ruvolo, P., Fabbri, G., Pasqualucci, L., Abdel-Wahab, O., & Rabadan, R. (2020). Mutations in the RNA Splicing Factor SF3B1 Promote Tumorigenesis through MYC Stabilization. Cancer discovery, 10(6), 806–821. https://doi.org/10.1158/2159-8290.CD-19-1330

Luukkonen, B. G., & Séraphin, B. (1997). The role of branchpoint-3' splice site spacing and interaction between intron terminal nucleotides in 3' splice site selection in Saccharomyces cerevisiae. The EMBO journal, 16(4), 779–792. https://doi.org/10.1093/emboj/16.4.779

Martinez Molina, D., Jafari, R., Ignatushchenko, M., Seki, T., Larsson, E. A., Dan, C., Sreekumar, L., Cao, Y., & Nordlund, P. (2013). Monitoring drug target engagement in cells and tissues using the cellular thermal shift assay. Science (New York, N.Y.), 341(6141), 84–87. https://doi.org/10.1126/science.1233606

Matera, A. G., & Wang, Z. (2014). A day in the life of the spliceosome. Nature reviews. Molecular cell biology, 15(2), 108–121. https://doi.org/10.1038/nrm3742

Maul-Newby, H. M., Amorello, A. N., Sharma, T., Kim, J. H., Modena, M. S., Prichard, B. E., & Jurica, M. S. (2022). A model for DHX15 mediated disassembly of A-complex spliceosomes. RNA (New York, N.Y.), 28(4), 583–595. https://doi.org/10.1261/rna.078977.121

Mizui, Y., Sakai, T., Iwata, M., Uenaka, T., Okamoto, K., Shimizu, H., Yamori, T., Yoshimatsu, K., & Asada, M. (2004). Pladienolides, new substances from culture of Streptomyces platensis Mer-11107. III. In vitro and in vivo antitumor activities. The Journal of antibiotics, 57(3), 188–196. https://doi.org/10.7164/antibiotics.57.188

Moteki, S., & Price, D. (2002). Functional Coupling of Capping and Transcription of mRNA. Molecular Cell, 10(3), 599–609. https://doi.org/10.1016/s1097-2765(02)00660-3

Mount, S. RNA processing: Sequences that signal where to splice. Nature 304, 309–310 (1983). https://doi.org/10.1038/304309a0

Nakajima, H., Sato, B., Fujita, T., Takase, S., Terano, H., & Okuhara, M. (1996). New antitumor substances, FR901463, FR901464 and FR901465. I. Taxonomy, fermentation, isolation, physico-chemical properties and biological activities. The Journal of antibiotics, 49(12), 1196–1203. https://doi.org/10.7164/antibiotics.49.1196

Nakajima, H., Takase, S., Terano, H., & Tanaka, H. (1997). New antitumor substances, FR901463, FR901464 and FR901465. III. Structures of FR901463, FR901464 and FR901465. The Journal of antibiotics, 50(1), 96–99. https://doi.org/10.7164/antibiotics.50.96

O'Day, C. L., Dalbadie-McFarland, G., & Abelson, J. (1996). The Saccharomyces cerevisiae Prp5 protein has RNA-dependent ATPase activity with specificity for U2 small nuclear RNA. The Journal of biological chemistry, 271(52), 33261–33267. https://doi.org/10.1074/jbc.271.52.33261

Papaemmanuil, E., Cazzola, M., Boultwood, J., Malcovati, L., Vyas, P., Bowen, D., Pellagatti, A., Wainscoat, J. S., Hellstrom-Lindberg, E., Gambacorti-Passerini, C., Godfrey, A. L., Rapado, I., Cvejic, A., Rance, R., McGee, C., Ellis, P., Mudie, L. J., Stephens, P. J., McLaren, S., Massie, C. E., … Chronic Myeloid Disorders Working Group of the International Cancer Genome Consortium (2011). Somatic SF3B1 mutation in myelodysplasia with ring sideroblasts. The New England journal of medicine, 365(15), 1384–1395. https://doi.org/10.1056/NEJMoa1103283

Plaschka, C., Lin, P. C., Charenton, C., & Nagai, K. (2018). Prespliceosome structure provides insights into spliceosome assembly and regulation. Nature, 559(7714), 419–422. https://doi.org/10.1038/s41586-018-0323-8

Query, C. C., McCaw, P. S., & Sharp, P. A. (1997). A minimal spliceosomal complex A recognizes the branch site and polypyrimidine tract. Molecular and cellular biology, 17(5), 2944–2953. https://doi.org/10.1128/MCB.17.5.2944

Quesada, V., Conde, L., Villamor, N., Ordóñez, G. R., Jares, P., Bassaganyas, L., Ramsay, A. J., Beà, S., Pinyol, M., Martínez-Trillos, A., López-Guerra, M., Colomer, D., Navarro, A., Baumann, T., Aymerich, M., Rozman, M., Delgado, J., Giné, E., Hernández, J. M., González-Díaz, M., … López-Otín, C. (2011). Exome sequencing identifies recurrent mutations of the splicing factor SF3B1 gene in chronic lymphocytic leukemia. Nature genetics, 44(1), 47–52. https://doi.org/10.1038/ng.1032

Reed R. (1989). The organization of 3' splice-site sequences in mammalian introns. Genes & development, 3(12B), 2113–2123. https://doi.org/10.1101/gad.3.12b.2113

Robert-Paganin, J., Réty, S., & Leulliot, N. (2015). Regulation of DEAH/RHA helicases by G-patch proteins. BioMed research international, 2015, 931857. https://doi.org/10.1155/2015/931857

Roybal, G. A., & Jurica, M. S. (2010). Spliceostatin A inhibits spliceosome assembly subsequent to prespliceosome formation. Nucleic acids research, 38(19), 6664–6672. https://doi.org/10.1093/nar/gkq494

Sakai, Y., Tsujita, T., Akiyama, T., Yoshida, T., Mizukami, T., Akinaga, S., Horinouchi, S., Yoshida, M., & Yoshida, T. (2002). GEX1 compounds, novel antitumor antibiotics related to herboxidiene, produced by Streptomyces sp. II. The effects on cell cycle progression and gene expression. The Journal of antibiotics, 55(10), 863–872. https://doi.org/10.7164/antibiotics.55.863

Seiler, M., Yoshimi, A., Darman, R., Chan, B., Keaney, G., Thomas, M., Agrawal, A. A., Caleb, B., Csibi, A., Sean, E., Fekkes, P., Karr, C., Klimek, V., Lai, G., Lee, L., Kumar, P., Lee, S. C., Liu, X., Mackenzie, C., Meeske, C., … Buonamici, S. (2018). H3B-8800, an orally available small-molecule splicing modulator, induces lethality in spliceosome-mutant cancers. Nature medicine, 24(4), 497–504. https://doi.org/10.1038/nm.4493

Selenko, P., Gregorovic, G., Sprangers, R., Stier, G., Rhani, Z., Krämer, A., & Sattler, M. (2003). Structural basis for the molecular recognition between human splicing factors U2AF65 and SF1/mBBP. Molecular cell, 11(4), 965–976. https://doi.org/10.1016/s1097-2765(03)00115-1

Shatkin, A. (1976). Capping of eucaryotic mRNAs. Cell, 9(4), 645–653. https://doi.org/10.1016/0092-8674(76)90128-8

Shen, J., Zhang, L., & Zhao, R. (2007). Biochemical characterization of the ATPase and helicase activity of UAP56, an essential pre-mRNA splicing and mRNA export factor. The Journal of biological chemistry, 282(31), 22544–22550. https://doi.org/10.1074/jbc.M702304200

Staley, J. P., & Guthrie, C. (1998). Mechanical devices of the spliceosome: motors, clocks, springs, and things. Cell, 92(3), 315–326. https://doi.org/10.1016/s0092-8674(00)80925-3

Topisirovic, I., Svitkin, Y. V., Sonenberg, N., & Shatkin, A. J. (2010). Cap and cap-binding proteins in the control of gene expression. Wiley Interdisciplinary Reviews: RNA, 2(2), 277–298. https://doi.org/10.1002/wrna.52

Uhlmann-Schiffler, H., Jalal, C., & Stahl, H. (2006). Ddx42p--a human DEAD box protein with RNA chaperone activities. Nucleic acids research, 34(1), 10–22. https://doi.org/10.1093/nar/gkj403

Wahl, M. C., Will, C. L., & Lührmann, R. (2009). The spliceosome: design principles of a dynamic RNP machine. Cell, 136(4), 701–718. https://doi.org/10.1016/j.cell.2009.02.009

Wan, Y., & Wu, C. J. (2013). SF3B1 mutations in chronic lymphocytic leukemia. Blood, 121(23), 4627–4634. https://doi.org/10.1182/blood-2013-02-427641

Wang, L., Lawrence, M. S., Wan, Y., Stojanov, P., Sougnez, C., Stevenson, K., Werner, L., Sivachenko, A., DeLuca, D. S., Zhang, L., Zhang, W., Vartanov, A. R., Fernandes, S. M., Goldstein, N. R., Folco, E. G., Cibulskis, K., Tesar, B., Sievers, Q. L., Shefler, E., Gabriel, S., … Wu, C. J. (2011). SF3B1 and other novel cancer genes in chronic lymphocytic leukemia. The New England journal of medicine, 365(26), 2497–2506. https://doi.org/10.1056/NEJMoa1109016

Wilkinson, M. E., Charenton, C., & Nagai, K. (2020). RNA Splicing by the Spliceosome. Annual review of biochemistry, 89, 359–388. https://doi.org/10.1146/annurev-biochem-091719-064225

Will, C. L., & Lührmann, R. (2011). Spliceosome structure and function. Cold Spring Harbor perspectives in biology, 3(7), a003707. https://doi.org/10.1101/cshperspect.a003707

Will, C. L., Urlaub, H., Achsel, T., Gentzel, M., Wilm, M., & Lührmann, R. (2002). Characterization of novel SF3b and 17S U2 snRNP proteins, including a human Prp5p homologue and an SF3b DEAD-box protein. The EMBO journal, 21(18), 4978–4988. https://doi.org/10.1093/emboj/cdf480

Wu, J., & Manley, J. L. (1989). Mammalian pre-mRNA branch site selection by U2 snRNP involves base pairing. Genes & development, 3(10), 1553–1561. https://doi.org/10.1101/gad.3.10.1553

Yan, C., Wan, R., Bai, R., Huang, G., & Shi, Y. (2016). Structure of a yeast activated spliceosome at 3.5 Å resolution. Science (New York, N.Y.), 353(6302), 904–911. https://doi.org/10.1126/science.aag0291

Yokoi, A., Kotake, Y., Takahashi, K., Kadowaki, T., Matsumoto, Y., Minoshima, Y., Sugi, N. H., Sagane, K., Hamaguchi, M., Iwata, M., & Mizui, Y. (2011). Biological

validation that SF3b is a target of the antitumor macrolide pladienolide. The FEBS journal, 278(24), 4870–4880. https://doi.org/10.1111/j.1742-4658.2011.08387.x

Yoshida, K., & Ogawa, S. (2014). Splicing factor mutations and cancer. Wiley interdisciplinary reviews. RNA, 5(4), 445–459. https://doi.org/10.1002/wrna.1222

Zamore, P. D., & Green, M. R. (1991). Biochemical characterization of U2 snRNP auxiliary factor: an essential pre-mRNA splicing factor with a novel intranuclear distribution. The EMBO journal, 10(1), 207–214. https://doi.org/10.1002/j.1460-2075.1991.tb07937.x

Zhang, Z., Will, C. L., Bertram, K., Dybkov, O., Hartmuth, K., Agafonov, D. E., Hofele, R., Urlaub, H., Kastner, B., Lührmann, R., & Stark, H. (2020). Molecular architecture of the human 17S U2 snRNP. Nature, 583(7815), 310–313. https://doi.org/10.1038/s41586-020-2344-3

Zhuang, Y. A., Goldstein, A. M., & Weiner, A. M. (1989). UACUAAC is the preferred branch site for mammalian mRNA splicing. Proceedings of the National Academy of Sciences of the United States of America, 86(8), 2752–2756. https://doi.org/10.1073/pnas.86.8.2752